THE JOURNAL OF BIOLOGICAL CHEMISTRY VOL. 287, NO. 19, pp. 15811–15825, May 4, 2012
Published in the U.S.A.

Three Acyltransferases and Nitrogen-responsive Regulator Are Implicated in Nitrogen Starvation-induced Triacylglycerol Accumulation in *Chlamydomonas*[*] [S]

Received for publication, December 18, 2011, and in revised form, March 7, 2012 Published, JBC Papers in Press, March 8, 2012, DOI 10.1074/jbc.M111.334052

Nanette R. Boyle[‡1], Mark Dudley Page[‡], Bensheng Liu[§], Ian K. Blaby[‡], David Casero[¶‖], Janette Kropat[‡], Shawn J. Cokus[¶], Anne Hong-Hermesdorf[‡], Johnathan Shaw[‡], Steven J. Karpowicz[‡2], Sean D. Gallaher[‡], Shannon Johnson[**], Christoph Benning[§], Matteo Pellegrini[¶‖], Arthur Grossman[‡‡3], and Sabeeha S. Merchant[‡‖4]

From the [‡]Department of Chemistry and Biochemistry, UCLA, Los Angeles, California 90095, the [§]Department of Biochemistry and Molecular Biology, Michigan State University, East Lansing, Michigan 48824, the [¶]Department of Molecular, Cell and Developmental Biology, UCLA, Los Angeles, California 90095, the [**]Genome Science, Los Alamos National Laboratory, Los Alamos, New Mexico 87545, the [‡‡]Department of Plant Biology, Carnegie Institution for Science, Stanford, California 94305, and the [‖]Institute of Genomics and Proteomics, UCLA, Los Angeles, California 90095

Background: Nitrogen-starvation and other stresses induce triacylglycerol (TAG) accumulation in algae, but the relevant enzymes and corresponding signal transduction pathways are unknown.
Results: RNA-Seq and genetic analysis revealed three acyltransferases that contribute to TAG accumulation.
Conclusion: TAG synthesis results from recycling of membrane lipids and also by acylation of DAG.
Significance: The genes are potential targets for manipulating TAG hyperaccumulation.

Algae have recently gained attention as a potential source for biodiesel; however, much is still unknown about the biological triggers that cause the production of triacylglycerols. We used RNA-Seq as a tool for discovering genes responsible for triacylglycerol (TAG) production in *Chlamydomonas* and for the regulatory components that activate the pathway. Three genes encoding acyltransferases, *DGAT1*, *DGTT1*, and *PDAT1*, are induced by nitrogen starvation and are likely to have a role in TAG accumulation based on their patterns of expression. *DGAT1* and *DGTT1* also show increased mRNA abundance in other TAG-accumulating conditions (minus sulfur, minus phosphorus, minus zinc, and minus iron). Insertional mutants, *pdat1-1* and *pdat1-2*, accumulate 25% less TAG compared with the parent strain, CC-4425, which demonstrates the relevance of the trans-acylation pathway in *Chlamydomonas*. The biochemical functions of *DGTT1* and *PDAT1* were validated by rescue of oleic acid sensitivity and restoration of TAG accumulation in a yeast strain lacking all acyltransferase activity. Time course analyses suggest than a *SQUAMOSA* promoter-binding protein domain transcription factor, whose mRNA increases precede that of lipid biosynthesis genes like *DGAT1*, is a candidate regulator of the nitrogen deficiency responses. An insertional mutant, *nrr1-1*, accumulates only 50% of the TAG compared with the parental strain in nitrogen-starvation conditions and is unaffected by other nutrient stresses, suggesting the specificity of this regulator for nitrogen-deprivation conditions.

Rising fossil fuel prices and dwindling reserves have led to renewed interest in developing alternative fuel sources (1–7). Although biomass from terrestrial plants can be processed and used as a feedstock for generating alcohols and other fuels (8) oil from photoautotrophically grown algae or seeds represents another fuel source, with algae offering distinct advantages over traditional oil crops (9, 10). The green alga *Chlamydomonas reinhardtii* accumulates increased amounts of triacylglycerols (TAGs)[5] under conditions of growth-inhibiting macro- or micronutrient deficiency such as sulfur (11), nitrogen (12–20), phosphorus (15), zinc, or iron deficiency (21) or other growth-inhibiting stressors such as high salt (22) or high light (23). With a sequenced genome (24) and the potential for application of metabolic engineering (25), *C. reinhardtii* is a powerful reference organism for discovering green algal TAG biosynthetic pathway(s) and the ways in which they are regulated by nutrient deprivation.

The lipid composition of *C. reinhardtii* is representative of a typical photosynthetic eukaryote with the notable exception that the betaine-containing lipid diacylglycerol-trimethyl-

* This work was supported, in whole or in part, by National Institutes of Health Grants T32 GM07185 and T32 ES015457 (to S. J. K. and I. K. B). This work was also supported by Air Force Office of Science Research Grants FA 9550-10-1-0095 (to S. M. and M. P.) and FA9550-08-0165 (to C. B.), Department of Energy Contract DE-EE0003046 (to the National Alliance for Advance Biofuels and Bioproducts Consortium, including S. M., M. P., and S. J.), and the German Academic Exchange Service Grant D/08/47579 (to A. H.).

[S] This article contains supplemental Tables S1–S7, Figs. S1–S13, and additional references.

The nucleotide sequence(s) reported in this paper has been submitted to the GenBank™/EBI Data Bank with accession number(s) JN815265 and JN815266.

[1] Present address: Dept. of Chemical and Biological Engineering, University of Colorado, Boulder, CO 80309.
[2] Present address: Dept. of Chemistry and Biochemistry, Eastern Oregon University, La Grande, OR 97850.

[3] Recipient of National Science Foundation Grants MCB-0951094 and MCB-0235878 for development and use of the mutant screen.

[4] To whom correspondence should be addressed: UCLA, 607 Charles E. Young Dr. E., Los Angeles, CA 90095. Tel.: 310-825-8300; Fax: 310-206-1035; E-mail: merchant@chem.ucla.edu.

[5] The abbreviations used are: TAG, triacylglycerol; DGAT, diacylglycerol acyltransferase; PDAT, phospholipid:diacylglycerol acyltransferase; nt, nucleotide; RPKM, reads per kilobase per million reads; TAP, tris acetate-phosphate; EST, expressed sequence tag; JGI, Joint Genome Institute.

homoserine replaces phosphatidylcholine in extraplastidic membranes (26). The genes associated with membrane lipid and TAG synthesis have been annotated in *Chlamydomonas*, relying primarily on BLAST analysis of the genome (1, 27). Nevertheless, the gene models tend to be incomplete, and function has not been established, especially in situations where multiple isoforms are predicted or where multiple metabolic routes exist.

Research in other eukaryotic organisms, such as yeast, *Arabidopsis*, and mouse, has identified several key genes in TAG synthesis. One is a diacylglycerol acyltransferase (DGAT), which catalyzes the final step in *de novo* TAG synthesis. The protein was identified in the mouse and was found to have sequence homology to sterol:acyl-CoA acyltransferase (28); DGATs of this type are now known as type-1 DGATs. Two other DGAT enzymes with little homology to type-1 DGATs were subsequently found in the oleaginous fungus *Morteriella ramanniana;* this type is classified as type-2 DGATs (29). Both type-1 and type-2 DGAT proteins are localized to the endoplasmic reticulum (30–32), and a study in *Vernicia fordii* (Tung tree) indicated that the two types of enzymes localize to different subdomains of the endoplasmic reticulum, implying nonredundant functions (33). Type-1 DGATs in plants are expressed in various cells and tissues, and type-2 DGATs are expressed highly in developing oilseeds (33–35), suggesting the importance of type-2 DGATs in TAG-accumulating organs. Likewise, type-2 DGAT in mouse is important since mice lacking this enzyme are severely depleted in both tissue and plasma TAG, which leads to early death (36). Genes representing a third class (type-3) of DGAT, which is a soluble cytosolic enzyme, have been identified in *Arachis hypogaea* (peanut) (37) and *Arabidopsis thaliana* (38).

Another major contributor to TAG synthesis is phospholipid:diacylglycerol acyltransferase (PDAT), which is an acyl-CoA independent enzyme that transfers the acyl group from the *sn*-2 position of a phospholipid to the *sn*-3 position of a diacylglycerol. In *Saccharomyces cerevisiae,* the two major contributors to TAG production in stationary and exponential cultures are type-2 DGAT and PDAT, respectively (encoded by *DGA1* and *LRO1*); two sterol acyltransferases (*ARE1* and *ARE2*) also contribute a small amount to the production of TAG (39, 40).

In *Chlamydomonas*, homology searches identified 5 type-2 DGATs, encoded by *DGTT1–DGTT5*. *DGTT1* is up-regulated in response to nitrogen starvation, but its function could not be validated (18, 41). Nevertheless, proteomic studies of membrane fractions from *Chlamydomonas* enriched for lipid droplets identified DGTT1, PDAT1, and a structural protein (named MLDP for major lipid droplet protein) (19, 42). To assess the role of these proteins in TAG accumulation in *Chlamydomonas*, we used RNA-Seq to describe the transcriptome during a time course of nitrogen starvation. The resulting coverage was used for annotation of *DGTT1* and *PDAT1* gene models, discovery, and annotation of a type-1 DGAT and a candidate transcription factor. The functions of DGTT1 and PDAT1 were validated by heterologous complementation in yeast, and the respective contributions of the enzymes encoded by *PDAT1* and of the candidate regulator were assessed in loss of function mutants.

EXPERIMENTAL PROCEDURES

Chlamydomonas Culture Conditions—C. reinhardtii strains CC-3269/2137 (wild-type *nit2 mt*$^+$), D66$^+$ (CC-4425 *nit2 cw15 mt*$^+$) (43, 44), *nrr1* (*nrr1 nit2 cw15 mt*$^+$), and *pdat1 (pdat1 nit2 cw15 mt*$^+$) were cultured at 24 °C (agitated at 180 rpm at a photon flux density of 90 μmol/m^2/s provided by cool white fluorescent bulbs at 4100 K and warm white fluorescent bulbs at 3000 K used in the ratio of 2:1) in tris acetate-phosphate (TAP) medium unless otherwise noted (45). Nutrient-deficient media were prepared as follows. NH_4Cl was omitted in nitrogen-free TAP; $MgSO_4$ was omitted in sulfur-free TAP; $ZnSO_4$ was replaced with $ZnCl_2$; potassium phosphate was replaced with 1 mM KCl in phosphorus-free medium (46); iron-free Hutner's trace element solution was supplemented with 0.25 μM $FeCl_3$ for low iron medium (47) and zinc-free Kropat's trace elements for zinc-deficient TAP medium (21).

Nitrogen Starvation Time Course Experiments—Several independent time course experiments of nitrogen starvation were performed to identify changes in transcript abundance at different time scales (0–1 h, 0–8 h, and 0–24 h). For each experiment, cells were grown in replete medium to a density of $\sim 4 \times 10^6$ cells ml^{-1}, collected by centrifugation (2170 $\times$ *g*, room temperature for 5 min), washed, and resuspended in nitrogen-free TAP medium to 2×10^6 cells ml^{-1}. For the 8-h time course, samples were taken at 0, 0.5, 4, and 8 h after transfer to nitrogen-free medium for RNA, chlorophyll, starch, and lipid analyses. The experiment was performed in triplicate. One of the three sets of RNA samples was used for RNA-Seq, and all three RNA samples were used for validation by real time PCR of cDNA. The first set of experiments indicated that some responses to nitrogen starvation occurred very quickly (<1 h), and others were much slower (>8 h). Therefore, two more time courses were performed. For the 48-h time course, samples were taken at 0, 2, 8, 12, 24, and 48 h after transfer to nitrogen-free medium. Independent cultures were grown in triplicate and were processed as described for the 8-h time course. A 1-h time course was also performed to capture the fast dynamics of nitrogen starvation response. Samples were taken before washing (0′) and at 0, 2, 4, 8, 12, 18, 24, 30, 45, and 60 min after transfer to nitrogen-free medium. This experiment was performed in duplicate, with one set of RNA samples used for RNA-Seq and both for validation by real time PCR of cDNA.

Nitrogen Limitation and Cell Density Experiments—For growth in reduced nitrogen, nitrogen-free TAP medium was supplemented with NH_4Cl to 7, 3.5, 1.75, 0.7, or 0.35 mM. Cultures of strain CC-3269 were inoculated to 1×10^5 cells ml^{-1} and collected for RNA at 1×10^6 cells ml^{-1}, when the growth rates of all cultures were identical. For assessing the impact of cell density, cultures were inoculated at 1×10^4 cells ml^{-1} in replete medium and sampled at 5×10^5 cells ml^{-1} and at each doubling thereafter until the culture reached a final density of 8×10^6 cells ml^{-1}.

Other Nutrient-deficient Experiments—Nitrogen-, sulfur-, or phosphorus-starved cells were grown to $\sim 4 \times 10^6$ cells ml^{-1}, collected by centrifugation (2170 $\times$ *g*, room temperature, 5 min), washed, and resuspended in the same medium to 2×10^6 cells ml^{-1} (46, 48). For iron or zinc deficiency, cells were grown

in the appropriate medium (1 μM Fe or 0 μM Zn) to generate an inoculum (2×10^4 cells ml^{-1}) for the experimental culture (49, 50). Sulfur- and phosphorus-deficient cultures were sampled for lipid analysis at 0 and 48 h after the cells were transferred to medium devoid of these nutrients; iron- and zinc-deficient cultures were collected at 3×10^6 and 5×10^6 cells ml^{-1}, respectively.

Saccharomyces Culture Conditions—*S. cerevisiae* strains BY4742 (wild type; *MATa his3Δ1 leu2Δ0 lys Δ0 ura Δ0*) and YPD1078 (*MATahis3Δ1 leu2Δ0 lys2Δ0 ura3Δ0 ycr048wΔ::KanMX4 ynr019wΔ::KanMX4 yor245cΔ::KanMX4 ynr008w Δ::KanMX4*), gifts from Sepp Kohlwein, University of Graz, were grown in YPD medium. Transformants were selected on a minimal medium containing 0.17% (w/v) yeast nitrogen base without amino acids, carbohydrate, or ammonium sulfate and 0.2% drop-out synthetic mix minus uracil (both US Biological), 0.5% (w/v) ammonium sulfate, 2% (w/v) dextrose, plus 1.5% (w/v) agar for solid medium. Counter-selection of the *ura3* marker was performed using 5′-fluoroorotic acid at a final concentration of 1 mg ml^{-1}. Functional complementation assays were performed on YPD agar containing oleic acid (0.009% w/v).

RNA Preparation and Analysis—Cells (50 ml) were collected by centrifugation (3440 × *g*, 5 min, 22 °C) and resuspended in 2 ml of water. Two ml of 2× lysis buffer was added, and the suspension was rocked for 20 min before it was flash-frozen in liquid N_2 and stored at −80 °C. Frozen samples were subsequently heated at 65 °C for 3 min, and RNA was extracted as described previously (51). The RNA concentration was measured on a NanoDrop 2000 (Thermo Scientific), and the quality of the RNA was assessed on an Agilent 2100 Bioanalyzer and by blot hybridization for *CBLP* (*RACK1*) mRNA (52). Other probes amplified from genomic DNA were for *PDAT1*, *DGTT1*, and *NRR1* (see supplemental Table S2 for primer sequences). Samples from the 8-h time course (0, 0.5, 2, 4, 6, and 8 h) and the 48-h time course (0, 0.5, 2, 4, 6, 8, 12, and 48 h) were pooled for generation of 454 EST tags at Joint Genome Institute (JGI). The data are deposited under accession SRX038871. The sequences were aligned to the reference 4.0 assembly and were visualized on a local installation of the UCSC browser. RNAs were also sequenced at Illumina and Los Alamos National Laboratory on a GAIIx system for estimating transcript abundance in nitrogen deficiency time course experiments or in cells grown in various amounts of ammonium supplements. Sequence data from a previous publication (18) were re-analyzed on the same pipeline for the purpose of comparison with the results presented here. The reads were aligned using bowtie (53) in single-end mode and with a maximum tolerance of three mismatches to the Au10.2 transcripts sequences, corresponding to the version 4.0 assembly of the *Chlamydomonas* genome. Expression estimates were obtained for each individual run in units of reads/kb of mappable transcript length/million mapped reads (RPKMs) (54) after normalization by the number of aligned reads and transcript mappable length (49).

DNA Gel Blot Hybridization—Genomic DNA was analyzed by hybridization as described previously (55). The probe used to detect the *AphVIII* cassette was the *AphVIII* ORF (805 bp) amplified from pSL18 (56) using primers *AphVIII*-F plus *AphVIII*-R (see supplemental Table S2), and *Pfx* DNA polymerase (Invitrogen) as directed by the manufacturer. The PCR product was isolated and labeled with [α-^{32}P]dCTP (57) to a specific activity of 2×10^9 dpm μg^{-1}. *Chlamydomonas* DNA-specific probes were produced by Klenow extension of overlapping 60-mer oligonucleotides (SP52-F and SP52-R; SP218-F and SP218-R; SPNR-F and SPNR-R, see supplemental Table S3) in the presence of [α-^{32}P]dCTP; probes had specific activities of 1×10^9 dpm μg^{-1}. Blots were exposed to film (Blue-sensitive X-ray; Henry Schein) at −80 °C using two intensifying screens.

Estimation of Relative mRNA Abundance—Complementary DNA synthesis and real time PCR were performed as described previously (50). Primers are listed in supplemental Table S4. Data are presented as the relative mRNA abundance and are normalized to the endogenous reference gene *CBLP* using LinRegPCR analysis (58, 59). Values were generated from three experimental replicates (for the 8-h experiment) and two experimental replicates (for the 1-h experiment); each replicate was analyzed three times (technical replicates). Real time reverse transcriptase PCR procedures and analyses follow the MIQE guidelines (60).

Sequencing of the DGAT1-containing BAC on the Illumina Platform—BAC REI35-B03 containing ~100 kb of *C. reinhardtii* DNA, including the *DGAT1* locus (a gift from Hudson Alpha Institute for Biotechnology, Huntsville, AL), was prepared from *Escherichia coli*. The DNA concentration was determined by Qubit dsDNA BR assay kit (Invitrogen). 100 ng of purified BAC DNA was sheared by the S-220 Adaptive Focused Acoustics system (Covaris, Woburn, MA) with the following conditions: 5% duty cycle, 20-watt peak incident power, 200 cycles/burst, 35 s. The ends of the resulting DNA fragments were repaired, and adaptors were ligated using reagents in the Illumina DNA TruSeq kit version 1 (Illumina, Inc. San Diego). At the gel isolation step, four bands of different sizes were isolated and purified according to the standard protocol. Individually, the four libraries of various sizes were subjected to 20 rounds of PCR amplification using the Illumina buffers, primers, and conditions. To determine the sizes of the four libraries, each was run on a BioAnalyzer DNA High Sensitivity chip (Agilent Technologies, Waldbronn, Germany). The four libraries (minus 126 nt for the Illumina adaptors) were 155, 335, 556, and 1014 nt long. The concentration of each was determined by Qubit dsDNA BR assay kit as before, and a 2 pM solution of each library was sequenced in 50 + 50-nt paired-end runs using the Illumina HiSeq 2000 platform with a TruSeq cBot PE cluster generation kit version 3. We obtained 6×10^5 raw reads (300,237 for 155 nt, 146,563 for 335 nt, 89,590 for 556 nt, and 62,318 for 1014 nt) with the correct Illumina adaptor sequence for a total of 6×10^7 base calls.

Gap-filling DGAT1 Sequence—The *DGAT1* gene model was built from the JGI version 3, 4, and 5 assemblies by re-assembly and filling of gaps in the vicinity with an iterative series of hand-directed analyses that relied on data from multiple sources, including dozens of Illumina RNA-Seq reads from this and other projects (GEO accession numbers GSE25124 and GSE35305), genomic DNA re-sequencing projects, and traces from the original JGI genome project (retrieved on March 15, 2011, by FTP to NCBI TraceDB) with manual re-calling of bases

in selected chromatograms. Tools included the following: ABySS (61) for *de novo* assemblies (both of genome and transcriptome) at both a whole genome/transcriptome level as well as targeted on select reads; traditional low throughput assembly/alignment tools; GMAP (62) numerous *ad hoc* assembly tools/analyses; BLAST and NCBI nonredundant nucleotide and protein databases; UCSC (63) and IGV (64) genome browsers; and manual inspection. Considerable additional sequence was recovered relative to the JGI version 3 and 4 assemblies; the gene model was refined, and the uncertainty is now restricted to the 5′ end of the transcript and its corresponding genomic sequence (see "Results"). The stretches of high C + G content (causing orders of magnitude drop in sequence coverage), tandem repeats in the vicinity, and inclusion of low complexity sequence in the coding region make sequencing very difficult by all sequencing technologies tried. PSI-BLAST analysis supports the model presented in this work, because protein sequence to the right of the gap aligns well with several type-1 DGAT sequences from oil-accumulating plants.

Lipid and Fatty Acid Analysis—For quantitative total fatty acid analysis, 5 ml of cell culture was collected on Whatman GF/A 25-mm circular glass filters, frozen in liquid nitrogen, and lyophilized. The filters (with cells) were transferred to reaction tubes and subjected to fatty acid methyl ester reactions and gas chromatography as described below. For TAG content, 20 ml of cell culture was collected by centrifugation (2170 × *g*, 2 min), washed in 1 ml of water, collected by centrifugation (13,780 × *g*, 5 min) in a 1.5-ml screw cap microcentrifuge tube, and frozen in liquid nitrogen. Prior to analysis, frozen cells were resuspended in 1 ml of methanol/chloroform/formic acid (2:1:0.1 (v/v/v)). Extraction solution (1 M KCl, 0.2 M H_3PO_4; 0.5 ml) was added and mixed by vortexing. Cell debris was removed by centrifugation for 3 min at 13,780 × *g*.

Lipids were separated by thin layer chromatography using petroleum ether/diethyl ether/acetic acid (8:2:0.1 (v/v/v)). Samples were run on baked Si60 silica plates (EMD Chemicals) for 5 min. After separation, lipids were reversibly stained by exposure to iodine vapor. The TAG band was located below pigments but above free fatty acid and DAG bands. TAG bands were quantitatively recovered by scraping the plate with a razor blade and transferring the material to a fatty acid methyl ester reaction tube. HCl in methanol (1 N, 1 ml) was added to each tube, and 5 μg of an internal standard (fatty acids 15:0, working concentration 50 μg/ml in methanol) was added. The head space in the tube was purged with nitrogen and the cap tightly sealed. Samples were incubated at 80 °C for 25 min and allowed to cool to room temperature. Aqueous NaCl (0.9%, 1 ml) and *n*-hexane (1 ml) were added, and the samples were shaken vigorously. After centrifugation at 1690 × *g* for 3 min, the hexane layer was removed, transferred to a new tube, and dried under a N_2 gas stream. The resulting fatty acid methyl esters were dissolved in 100 μl of hexane. Fatty acid content and composition of the extracts were determined by gas chromatography with flame ionization detection, as described previously (65). The capillary DB-23 column (Agilent) was operated as follows: initial temperature 140 °C, increased by 25 °C/min to 160 °C, then by 8 °C/min to 250 °C, and held at 250 °C for 4 min.

Gene Model Verification—Gene models were derived by adjusting FM4 and Au5 models based on 454 ESTs (SRA020135) and verified experimentally by amplification of cDNAs and sequencing (Beckman Coulter Genomics, Danvers, MA). Primers used for this can be found in the supplemental material. The latest release of *Chlamydomonas* gene models Au10.2 at Phytozome includes these adjustments.

Microscopy—*Chlamydomonas* and yeast (1 ml from the culture) were stained with Nile Red® (Sigma) by adding the dye to a final concentration of 1 mg/ml and agitating the suspension for 5 min. Cells were collected by centrifugation (1000 × *g*, 2 min), resuspended in 200 μl of the growth medium, and immobilized by 1:1 mixing with 1.5% low melting agarose (total volume of 16 μl). Images were acquired with a Leica TCS-SPE confocal microscope using an APO ×63.0 water objective with a numerical aperture of 1.15. The Nile Red® signal was captured using a laser excitation line at 488 nm, and emission was collected between 554 and 599 nm (gain, 700; offset, 0). Chlorophyll autofluorescence was excited at 635 nm and captured between 670 and 714 nm. Differential interference contrast images were acquired in the PM Trans channel (gain, 371; offset, 0). Images were colored using Leica confocal software.

Generation and Screening of Chlamydomonas Mutants—A library of 25,000 insertional mutants in CC-4425 ($D66^+$), created by insertion of a 1.7-kb PCR fragment containing the selectable marker gene *AphVIII* (66), was prepared as described previously (67). Screening for mutants was performed according to González-Ballester (68). Briefly, transformants picked from selective agar were transferred to 96-well microtiter plates containing 100 μl of TAP medium. Plates were wrapped in parafilm to minimize evaporation and grown for 5 days. Aliquots from the wells of each plate were pooled so that each pool represented the 96 mutants on one plate. Genomic DNA was isolated using the standard phenol/chloroform method (69). Equal amounts of genomic DNA from each of 10 pools were combined to create a "superpool" of DNA at a final concentration of 100 ng/μl. To screen for mutants with inserts in genes of interest, the superpool DNA was used as the template for PCR. Each PCR was performed using a gene-specific primer (the gene for which a disruption is sought; see supplemental Table S5) and an *AphVIII* construct-specific primer (RB2, 5′-TACCGGCTGTTGGACGAGTTCTTCTG-3′). A number of gene-specific primers, annealing at different positions within the target gene, were employed (listed in supplemental Table S5).

PCRs (final volume 25 μl) contained 0.5 unit of *Taq*DNA polymerase (Qiagen), 1× PCR buffer, 1× "Q" solution, DMSO (5% v/v), dNTPs (200 μM each), primers (300 nM each), and pooled genomic DNAs (100 ng). Template DNA was denatured for 5 min at 95 °C followed by amplification (30 s at 95 °C, 45 s at 60 °C, and 2 min at 72 °C, 40 cycles). PCR products were separated by electrophoresis in 1% agarose gels. To identify DNA regions adjacent to the right border of the *AphVIII* construct, PCR products were isolated (QIAquick gel extraction kit, Qiagen) and sequenced. Once a positive clone in a superpool was identified, the PCR screen was used to determine the specific microtiter plate and then the row and column within that plate associated with the mutant strain of interest; this localizes the mutant to a single well.

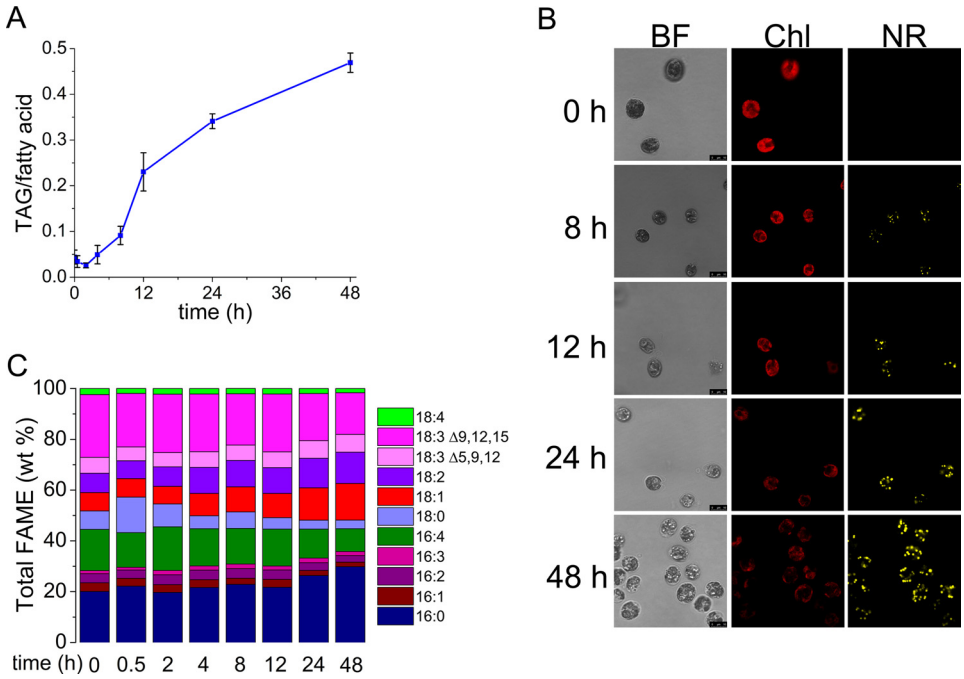

FIGURE 1. **Time course of increased TAG accumulation in nitrogen-starved *C. reinhardtii* wild type (CC-3269) cells.** *A,* fraction of fatty acids in TAG in nitrogen-starved cells during a 48-h time course of nitrogen starvation on a mol/mol basis. *Error bars* represent standard deviation from three biological replicates. Two-tailed Student's *t* test on experimental triplicates for each time point indicate that 8-, 12-, 24-, and 48-h samples are statistically different from the 0-h sample at 98% confidence. *B,* confocal microscopy of nitrogen-starved cells to visualize TAG by Nile Red staining. *BF,* bright field; *Chl,* chlorophyll autofluorescence; *NR,* Nile Red fluorescence. *C,* fatty acid composition of lipids at each time point was measured by gas chromatography; the average of three experimental replicates is shown. Microscopy of cells in replete medium is given in supplemental Fig. S3.

PCR Analysis of AphVIII Cassette Insertion Structures in Mutant Lines—Amplification across the 5′ side junction between the *AphVIII* cassette and *Chlamydomonas* genomic DNA in mutant *pdat1-1* was performed using primers PDAT1-1-F1 plus RIM5-2 (supplemental Table 5). Reactions contained 1× ThermalAce buffer (Invitrogen), dNTPs (160 μM each), primers (0.5 μM each), genomic DNA (100 ng), and *Taq* (1 unit). Template DNA was denatured for 5 min at 95 °C followed by amplification (30 s at 95 °C, 30 s at 55 °C, and 60 s at 72 °C, 36 cycles). The PCR product was isolated and sequenced using primers PDAT1-1-F1 and RIM5-2. Amplification across the *AphVIII* cassette in mutant *pdat1-2* was performed using primers PDAT1-2-F1 plus PDAT-SR7, and Phusion DNA polymerase (Finnzymes) as directed by the manufacturer. Reactions contained 1× GC buffer, DMSO (3% v/v), dNTPs (300 μM each), primers (0.5 μM each), genomic DNA (100 ng), and polymerase (1 unit). Template DNA was denatured for 30 s at 98 °C followed by amplification (10 s at 98 °C and 155 s at 68 °C, 30 cycles). The PCR product was isolated and sequenced using primer PDAT1-2-F1. Location of the insert is shown in supplemental Table S6.

Plasmid Construction—Plasmids were introduced into and amplified in *E. coli* XL1-Blue (*endA1 gyrA*96(nal^R) *thi-1 recA1 relA1 lac gln*V44 F′[::*Tn*10 *proAB*$^+$ *lacI*^{q} Δ(*lacZ*)M15] *hsdR17*(r_K^- m_K^+). Synthetic genes encoding DGTT1 and PDAT1 were codon-optimized for expression in *S. cerevisiae* by GenScript (Piscataway, NJ). The sequences are shown in supplemental Figs. S1 and S2 and a codon use table is provided in supplemental Table S7. Codon-optimized genes were cloned in pUC57 (GenScript, Piscataway, NJ) and subsequently subcloned into the *Spe*I and *Xho*I sites of pGPD417-LNK to generate pIKB506 and pIKB507. pIKB505 was generated by amplifying *LRO1* from purified *S. cerevisiae* genomic DNA using primers 5′-ACGTAGAATTCATGGGCACACTGTTTCGAAGA-3′ and 5′-ACGTAGCATGCTTACATTGGGAAGGGCATCTGAG-3′ and inserted (after digestion) between the *Eco*RI and *Sph*I sites of pCGCU. Plasmids were introduced into *S. cerevisiae* and selected on the basis of uracil prototrophy or kanamycin resistance as appropriate.

RESULTS

Time Course of TAG Accumulation—Several stress conditions promote the accumulation of TAG-containing lipid bodies in *Chlamydomonas* (11–15, 17–19, 21, 70). To identify changes in gene expression associated with TAG accumulation, we sought to analyze the transcriptome under nitrogen starvation conditions because it is the most effective inducer of TAG accumulation. To identify suitable time points for transcriptome analysis, we monitored TAG accumulation in a time course following transfer of wild-type cells from nitrogen-replete to nitrogen-deficient conditions (Fig. 1). Quantitative gas chromatography indicates that the fraction of fatty acids (out of total per cell) associated with TAG is noticeably increased at 8 h of starvation and continues to increase through 48 h (Fig. 1*A*). Student's *t* test indicates that 8-, 12-, 24-, and 48-h samples are statistically different from the 0-h sample with 98% confidence. This agrees well with confocal fluorescence microscopy, which shows increased abundance of Nile Red-stained lipid bodies with a concomitant decrease in chlorophyll fluorescence (Fig. 1*B*). In contrast, the replete cells did not accumulate Nile Red staining bodies (supplemental Fig. S3). Composition analysis indicates that there is a progressive

TABLE 1

Nitrogen starvation impacts many genes associated with fatty acid metabolism

Many genes involved in glycerolipid metabolism were identified previously (18, 27, 72). Genes without functional annotation are indicated with Au10.5 and Au5 transcript IDs.

Au10.2	Au5	Gene name	Description	RPKM				
				0 h	2 h	12 h	24 h	48 h
Cre12.g519100	513248	*ACX1*	α-Carboxyltransferase	140.5	68.2	81.3	71.6	70.2
Cre12.g484000	512497	*BCX1*	β-Carboxyltransferase	103.5	53.4	35.1	35.4	31.4
Cre17.g715250	517403	*BCC1*	Acetyl-CoA biotin carboxyl carrier	293.9	129.6	54.7	74.7	68.9
Cre01.g037850	511392	*BCC2*	Acetyl-CoA biotin carboxyl carrier	271.5	89.8	43.9	55.9	58.1
Cre01.g063200	511929	*ACP1*	Acyl carrier protein	211.0	220.6	171.6	157.3	113.7
Cre13.g577100	514476	*ACP2*	Acyl carrier protein	3513.1	1740.6	1110.7	1777.4	1399.1
Cre16.g656400	516156	*SQD1*	UDP-sulfoquinovose synthase	119.4	88.4	36.7	49.8	61.7
Cre01.g038550	511409	*SQD2*	Sulfoquinovosyldiacylglycerol synthase	10.3	7.6	3.4	6.7	2.1
Cre16.g689150	516856	*SQD3*	Sulfoquinovosyldiacylglycerol synthase	0.3	0.4	0.0	0.0	0.0
Cre13.g585300	514645	*MGD1*	Monogalactosyldiacylglycerol synthase	16.1	1.4	6.3	5.3	3.4
Cre13.g583600	514612	*DGD1*	Digalactosyldiacylglycerol synthase	29.0	31.2	52.4	42.5	36.4
Cre06.g250200	522823	*SAS1*	*S*-Adenosylmethionine synthetase	2334.8	1167.6	283.0	401.4	578.3
Cre07.g324200	524437	*BTA1*	Diacylglyceryl-*N*,*N*,*N*-trimethylhomoserine synthesis protein	120.1	129.7	82.5	79.1	68.6
Cre12.g539000	513669	*ECT1*	CDP-ethanolamine synthase	17.4	20.7	25.2	17.1	16.9
Cre03.g162600	520698	*PGP3*	Phosphatidylglycerolphosphate synthase	7.3	6.6	1.4	2.8	4.8
Cre03.g180250	521070	*INO1*	Myoinositol-1-phosphate synthase	194.9	158.7	305.3	282.2	188.5
Cre10.g419800	509612	*PIS1*	Phosphatidylinositol synthase	29.5	22.6	27.0	29.2	26.9
Cre14.g621650	515418	*MCT1*	Malonyl-CoA:acyl carrier protein transacylase	159.9	137.8	35.2	10.8	19.7
Cre01.g045900	511566	*DGAT1*	Diacylglycerol acyltransferase, DAGAT type-1	3.3	11.7	15.0	9.1	20.8
Cre12.g557750	514063	*DGTT1*	Diacylglycerol acyltransferase, DAGAT type-2	0.8	7.9	11.1	17.5	24.6
Cre02.g121200	519435	*DGTT2*	Diacylglycerol acyltransferase, DAGAT type-2	22.2	21.1	24.5	26.2	26.8
Cre06.g299050	523869	*DGTT3*	Diacylglycerol acyltransferase, DAGAT type-2	35.5	33.4	31.5	40.7	32.5
Cre03.g205050	521604	*DGTT4*	Diacylglycerol acyltransferase, DAGAT type-2	4.6	7.5	7.5	2.9	3.3
Cre02.g079050	518531	*DGTT5*	Diacylglycerol acyltransferase, DAGAT type-2	0.0	0.0	0.1	0.0	0.0
Cre02.g106400	519119	*PDAT1*	Phospholipid diacylglycerol acyltransferase	3.4	9.4	8.5	9.7	8.0

increase in saturated and mono-unsaturated fatty acids (16:0 and 18:1) and a decrease in the proportion of polyunsaturated ones (16:4, 18:3) (Fig. 1*C*). After 48 h of starvation, the total amount of saturated fatty acids was 20% more (w/w) than at 0 h.

Using the rationale that changes in mRNA abundance should precede changes in TAG accumulation, we isolated RNA for transcriptome analysis in three time course experiments as follows: 0–1 h, 0–8 h, and 0–48 h following transfer of cells from nitrogen-replete to nitrogen-deficient medium, referred to subsequently as short, medium, and long time courses. For the short time course, we sampled cells at two "reference" zero points: one labeled 0′, corresponding to the nitrogen-replete cells at a density of 4×10^6 cells ml^{-1}, and the other labeled 0, corresponding to nitrogen-replete cells just immediately after centrifugation and transfer to fresh nitrogen-free medium at a density of 2×10^6 cells ml^{-1} (see under "Experimental Procedures"). This allowed us to distinguish changes related to the handling of cells from changes resulting from nitrogen starvation. RNAs were analyzed by sequencing (Illumina platform) and by real time PCR on cDNA generated by reverse transcriptase for validation of changes in abundance of select mRNAs (see under "Experimental Procedures").

Impact on Fatty Acid and Lipid Synthesis—We augmented the existing annotations (27, 71, 72) of genes corresponding to enzymes involved in fatty acid and membrane and neutral lipid biosynthesis and queried the abundance of the corresponding mRNAs (select genes and time points given in Table 1, for all time points see supplemental Table S1). We noted that with the exception of a putative palmitoyl-protein thioesterase-encoding gene (Cre01.g067300), which may function to liberate fatty acids for lipid/TAG synthesis and whose expression is increased nearly 3-fold, most of the genes (*ACX1*, *ACX2*, *BCC1*, *BCC2*, *ACP1*, and *ACP2*) encoding enzymes (carboxyltransferases, acetyl-CoA biotin carboxyl carrier, acyl carrier protein, malonyl-CoA-acyl carrier protein transacylase) in *de novo* fatty acid synthesis, as well as genes (*SQD1*, *SQD2*, *MGD1*, *DGD1*, *SAS1*, *BTA1*, *ECT1*, *PGP3*, *INO3*, and *PIS1*) encoding functions in membrane lipid synthesis, are down-regulated. One of the most dramatic changes is in Cre14.g621650 mRNA (a malonyl-CoA-acyl carrier protein transferase), whose abundance decreased from 160 RPKM to 19.7 RPKM at 48 h of nitrogen starvation.

Surprisingly, genes *LIPG2*, Cre05.g234800, and Cre02.g127300, encoding candidate TAG lipases, are up-regulated, which has also been noted in previous transcriptome and proteome studies (18, 42). One possibility is that these enzymes are not TAG lipases but rather play a role in releasing fatty acids from membrane lipids for *de novo* TAG synthesis. Membrane recycling has been reported to supply ~30% of TAG accumulation during nitrogen starvation (73). Several other candidate lipases are down-regulated, such as *LIPG1*, Cre10.g422850, and Cre05.g248200, and these may represent the authentic TAG lipases instead.

The expression of genes encoding various desaturases is either unchanged or decreased in nitrogen starvation conditions. *DES6*, one of the most abundant mRNAs in *Chlamydomonas* (rank 88 of 17,303 in nitrogen-replete cells) is decreased 7-fold at 48 h. *FAD5a* mRNA shows a similar 6.6-fold decrease, with a 1.6-fold decrease noted as early as 2 h after initiation of nitrogen starvation. These changes are consistent with the observation that the level of saturation of fatty acids is increased in response to nitrogen starvation (Fig. 1*C*).

Three Acyltransferases with Increased Expression—Three different DGAT enzymes are found in plants, two are membrane-associated and a third is soluble. The membrane-associated DGATs are of two types; the one corresponding to the DGAT1 gene family is related to the mammalian DGAT enzyme, and the others are similar to the steryl acyltransferases

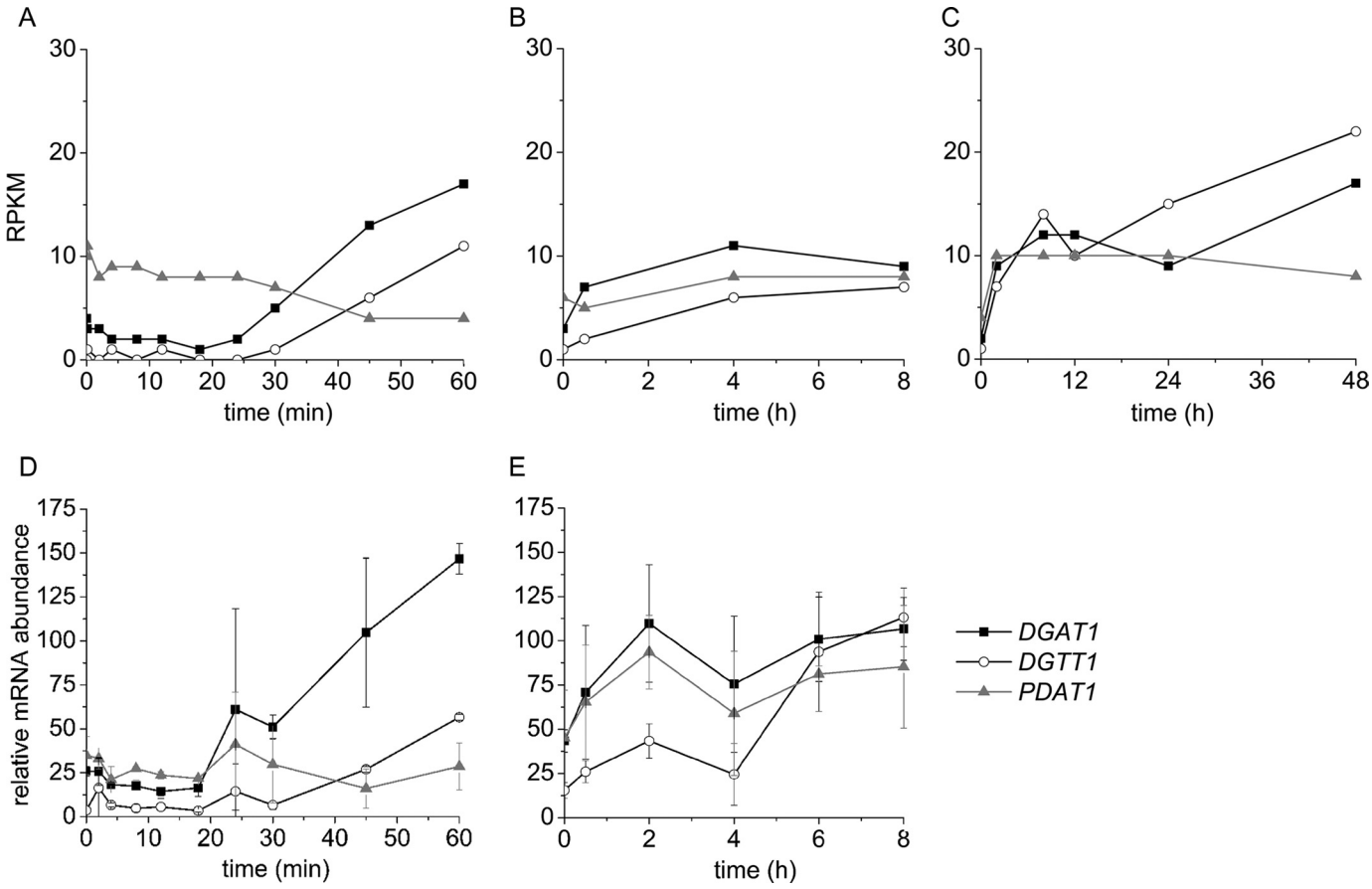

FIGURE 2. **Increased expression of *DGAT1, DGTT1,* and *PDAT1* encoding three nitrogen deficiency-responsive acyltransferases.** mRNA abundance was reported in RPKM in a 1-h time course (*A*), 8-h time course (*B*), and 48-h time course (*C*) after the onset of nitrogen starvation. Relative mRNA abundance in a 1-h time course (*D*) and 8-h time course (*E*) was measured by real time PCR. *Error bars* on *D* and *E* are standard deviations from two biological samples analyzed in technical triplicate.

Are1p/Are2p from *S. cerevisiae* and a distinct type-2 family that encodes enzymes related to the *S. cerevisiae* Dga1p. In *Chlamydomonas*, these genes are named *DGTT* for diacylglycerol acyltransferase type-2. The function of the third soluble enzyme has not been investigated.

Of the five previously annotated *DGTT* genes, *DGTT1* is the only one responsive to nitrogen starvation. *DGTT2* and *DGTT3* are expressed at moderate levels, and these levels remain approximately constant over the time courses of the experiments presented here. *DGTT4* mRNA abundance is low (about 10–20% relative to *DGTT2* and *DGTT3*), and *DGTT5* expression has not been detected. These findings agree with a previous study of the response of *Chlamydomonas* to nitrogen starvation (18). The increase in *DGTT1* mRNA is noted between 30 and 60 min of nitrogen starvation, and the level remains high for up to 48 h (Fig. 2, *A–C*). Patterns of expression noted in the mRNA-Seq analysis were validated in RNAs isolated up to 8 h after nitrogen starvation by real time PCR of cDNAs in triplicate experiments (Fig. 2, *D* and *E,* and supplemental Fig. S4). After 8 h of nitrogen starvation, nearly all transcripts were changed in abundance, and therefore we were unable to find a suitable "control" gene. Nevertheless, the magnitude of the increase in expression at 48 h is similar to the increase noted in previous work relative to the replete condition, time 0 (see Table 1) (18).

In addition to *DGTT1*, we noted increased expression of a gene, which we named *DGAT1*, that encodes a type-1 DGAT (Fig. 2). This sequence was not annotated in previous assemblies of the *Chlamydomonas* genome because of a large sequence gap that obscured the 5′ half of the gene model. The pattern of expression of *DGAT1* is very similar to that of *DGTT1*, which motivated us to improve the assembly (see "Experimental Procedures"). The sequence information now covers ~90% of the locus (sequence is given in supplemental Fig. S5 and predicted protein structure is given in supplemental Fig. S6). Nevertheless, the region is refractory to amplification and cloning, and two small gaps remain in the predicted coding region (see supplemental Figs. 5 and 6). In terms of absolute abundance, *DGTT1* and *DGAT1* mRNAs are approximately the same, and they attain levels that are comparable with those observed for *DGTT2* and *DGTT3*, whose levels are already high in nitrogen-replete cells and remain high throughout the time course (Table 1). In photoautotrophic cells, *DGTT3* and *DGTT4* mRNAs are also increased in nitrogen deficiency (74).

A third acyltransferase, which we named PDAT1 because of orthology to *Arabidopsis* PDAT1, also shows a small but reproducible increase in abundance in nitrogen-starved cells. In contrast to *DGAT1* and *DGTT1,* whose mRNAs increase progressively throughout the 48-h time course, the increase in *PDAT1* mRNA plateaus by 2 h. This may be related to the cell density-

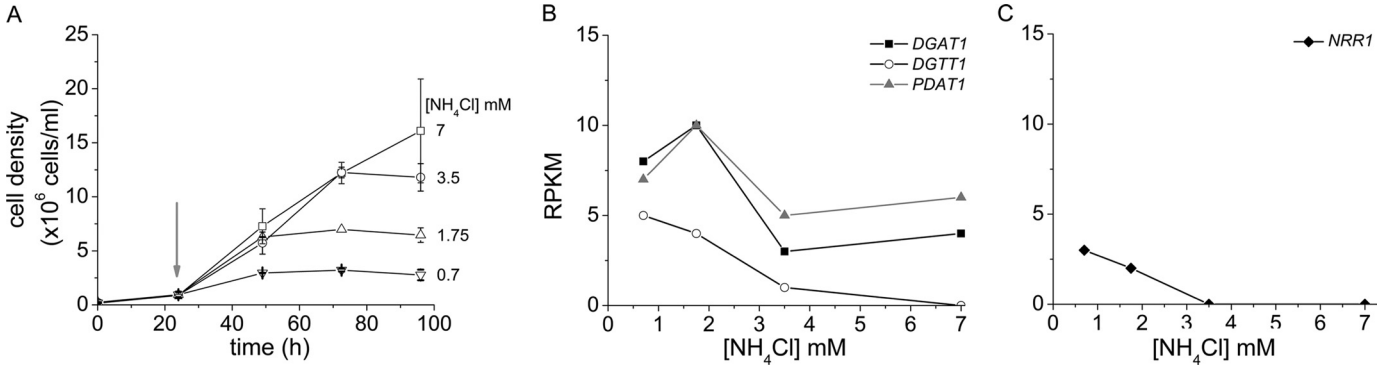

FIGURE 3. **Impact of nitrogen nutrition on cell growth (*A*) and mRNA abundance of *DGAT1*, *DGTT1*, and *PDAT1* (*B*), and *NRR1* (*C*).** *Chlamydomonas* cells were grown with various amounts of ammonium chloride (see under "Experimental Procedures"), and RNA was sampled at a cell density of 1×10^6 cells ml^{-1} (indicated with an *arrow*) when cells were still growing at the same rate.

dependent decrease in *PDAT1* mRNA abundance (supplemental Fig. S8). Increases in *DGAT1* and *PDAT1* mRNA were verified by real time PCR of cDNAs (Fig. 2, *D* and *E*) and also by blot hybridization (supplemental Fig. S7).

In a separate experiment, we monitored transcript abundance in cells acclimated to low nitrogen content. *Chlamydomonas* cells were washed with nitrogen-free medium and inoculated into medium supplemented with various amounts of NH_4Cl (up to 7 mM, which is the concentration in TAP medium). Cells were grown to a density of 1×10^6 cells ml^{-1} prior to collecting the cells for RNA isolation. Because the cells grew at approximately the same rate up to this point, independent of NH_4Cl concentration, this corresponded to about four divisions for each culture. When we monitored transcript abundance for the three acyltransferases, we noted that all three respond to low nitrogen content and that the abundances of *PDAT1* and *DGAT1* mRNAs were very similar, again suggesting that these three enzymes are responding to nitrogen deficiency (Fig. 3). In contrast, in these same experiments the amounts of *DGTT2* and *DGTT3* mRNAs appear to be independent of nitrogen content of the medium.

Because limitation for several different nutrients can promote TAG accumulation (11–15, 17–19, 21, 70), we tested whether low concentrations of a variety of different nutrients impact *DGTT1*, *DGAT1*, and *PDAT1* expression (Fig. 4). *DGTT1* mRNA increased under each nutrient limitation condition tested (minus sulfur, minus phosphorus, minus zinc, and low iron), although not to the same extent as during nitrogen starvation, which correlates with the relative amounts of TAG accumulated in each condition. Similar to *DGTT1*, *DGAT1* is also up-regulated when the cells are limited for the nutrients tested in this experiment, with the exception of phosphorus deprivation, suggesting that at least some distinct signaling pathways may impact acyl-CoA-dependent TAG synthesis pathways and validating the relevance of both these enzymes in TAG biosynthesis. The *PDAT1* transcript, however, only increases in nitrogen-starved cells. This may mean that fatty acid recycling from membrane lipids into TAG is more relevant in a subset of stress conditions or that PDAT activity can also be controlled by post-transcriptional processes in other stress situations.

Nitrogen Response Regulator—To identify candidate regulators of nitrogen deficiency-induced TAG accumulation, we searched among the differentially expressed RNAs for those encoding proteins with DNA binding domains. One transcript was of particular interest because of the magnitude of its regulation and co-expression with the *DGTT1* mRNA (Fig. 5*A*). The gene model, which was named *NRR1* for nitrogen response regulator, was manually curated based on RNA-Seq and 454 EST coverage (Fig. 6) and verified by sequencing (supplemental Fig. S9). A *SQUAMOSA* promoter-binding protein domain, named for its occurrence in the founding member (the SQUAMOSA promoter-binding protein), is predicted at its N terminus, and the *SQUAMOSA* promoter-binding protein domain is conserved in other algae and plants (supplemental Fig. S10). When we examined the abundance of the *NRR1* transcript in other TAG-accumulating conditions, we found that the increase is specific for the nitrogen starvation response (Fig. 5*B*, for a larger version see supplemental Fig. S11). The gene is also expressed in cells acclimated to low nitrogen (Fig. 3*C*). Changes in mRNA abundance were validated by real time PCR of cDNA in triplicate experiments (supplemental Fig. S4).

Functional Validation—Because the gene models (FM4 or Au5 on the JGI browser) for the version 4 assembly of the *Chlamydomonas* genome were largely computationally derived and based only on a few hundred thousand Sanger-sequenced ESTs, we used EST data derived from a pooled sample of RNA from nitrogen-deficient cells (see under "Experimental Procedures") and other recently obtained 454 ESTs to curate the gene models (Fig. 6). The manually curated models (Fig. 6, *blue*) are consistent with the RNA-Seq coverage graphs that show increased expression of each exon in nitrogen deficiency (see *DGTT1* and *NRR1* loci in particular). Each model was validated by sequencing the entire cDNA (*e.g.* for *PDAT1*) or by sequencing amplified regions of the cDNAs across exon-exon junctions (supplemental Fig. S7). For *DGTT1*, we noted the inclusion of an additional exon at the 5′ end, which is likely important for function (*circled* in Fig. 6). For *PDAT1*, the size of the transcript predicted for the revised model matches well with the size ($\sim 3.6 \times 10^2$ nt) estimated from blot hybridization (supplemental Fig. S2). The new models are included in the latest set of Au10.2 gene models at Phytozome, which also relies on the 454 ESTs.

We tested the biochemical activities of *DGTT1* and *PDAT1* in a heterologous system by complementation of an *S. cerevisiae* mutant carrying a quadruple deletion in four acyltransferases

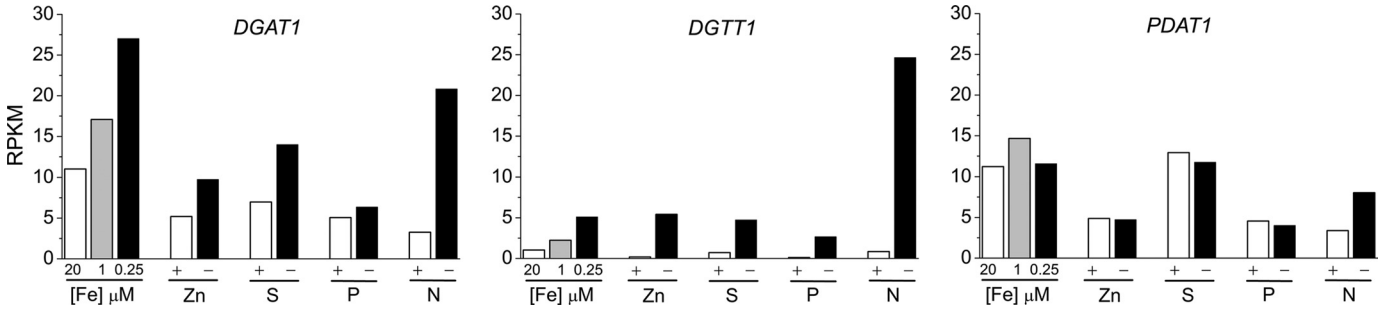

FIGURE 4. **Response of *DGAT1*, *DGTT1*, and *PDAT1* mRNA abundance to other TAG-accumulating conditions.** Cells were grown in TAP medium under replete (20 μM iron, zinc, sulfur, phosphorus, and nitrogen), deficient (1 or 0.25 μM iron), or nutrient starvation (minus zinc, minus sulfur, minus phosphorus, and minus nitrogen) conditions as described under "Experimental Procedures." mRNA abundance is expressed in RPKM.

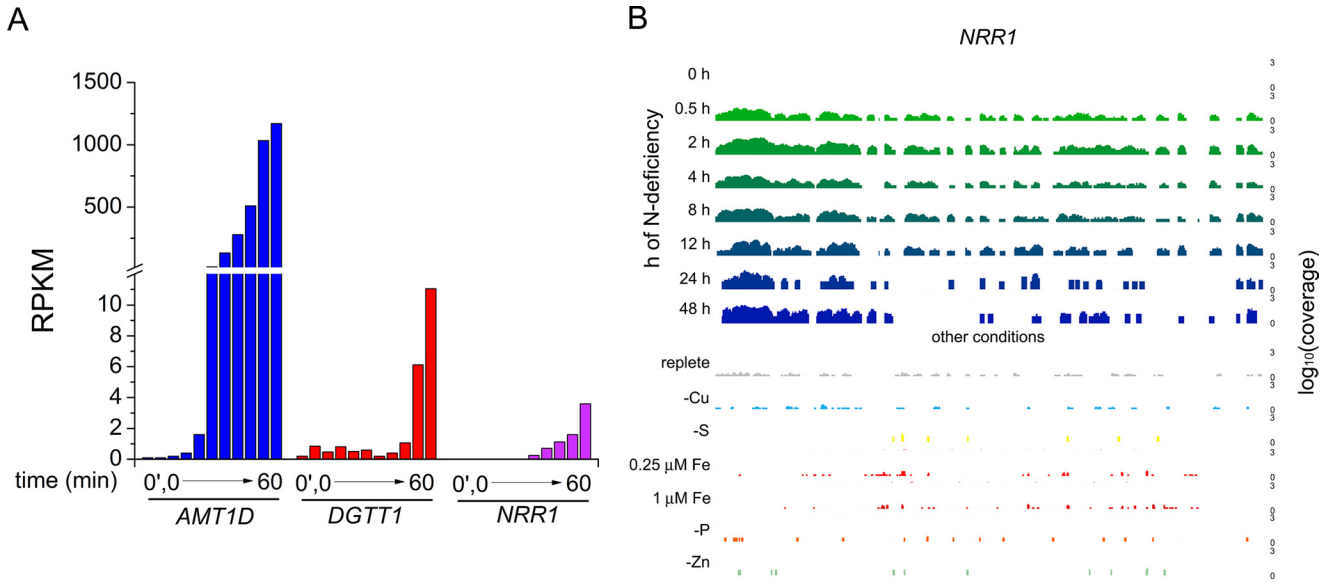

FIGURE 5. **Pattern of expression of the nitrogen-responsive regulator, *NRR1*.** *A*, mRNA abundance of an ammonium transporter *AMT1D*, an acyltransferase *DGTT1*, and *NRR1*. *B*, browser view of the *Chlamydomonas NRR1* locus; nitrogen starvation mRNA abundance is shown at the top (0–48 h) and other conditions (replete, minus copper, and minus sulfur, 0.25 μM iron, 1 μM iron, minus phosphorus, and minus zinc sampled as described under "Experimental Procedures") are below. Note that the *y* axis, representing absolute expression (RPKM) is presented on a $\log_{10}$ scale (0–3 in each case, covering 3 orders of magnitude); the differences in RNA abundance between minus nitrogen and the other deficiency conditions is substantial. A larger version of this figure is shown in supplemental Fig. S11, and the complete data set is available via the UCSC browser on line.

(encoded by *DGA1*, *LRO1*, *ARE1*, and *ARE2*) that contribute to TAG synthesis (75). The resulting strain is sensitive to oleic acid, and introduction of either a DGAT- or PDAT-encoding sequence will rescue the strain (76). Codon-optimized versions of *Chlamydomonas DGTT1* and *PDAT1* were tested for function in this assay and indeed render the mutant resistant to oleic acid (Fig. 7). When we stained the yeast strains with Nile Red, only strains complemented with acyltransferases showed lipid body accumulation, validating the function of these enzymes. When the complementing plasmids were cured by 5′-fluoroorotic acid counter-selection, the strains regained the oleic acid sensitivity phenotype establishing a causal connection.

Reverse Genetic Validation—We took advantage of a collection of insertional mutants to identify candidate loss of function alleles in *PDAT1* and *NRR1* by PCR (67, 68). The position of the inserts was verified by sequencing PCR products from the 3′ side insertion junction; in *pdat1-1* the *AphVIII* cassette is integrated in the 12th exon, in *pdat1-2* in the 6th intron, and in *nrr1-1* in the 7th exon (Fig. 8*A*). Sequencing across the 5′ side insertion junctions in the *pdat* mutants indicates that the integration events were accompanied by no or minimal deletion of *Chlamydomonas* DNA (0 bp in *pdat1-2* and 4 bp in *pdat1-1*) (supplemental Fig. S1). Southern blotting verified that each mutant carries a single copy of the cassette per genome and also verified the position of the integrated DNA in each of the mutants (supplemental Fig. S4). For *nrr1*, we used multiple gene-specific probes to demonstrate that the insertion is not accompanied by a large deletion at the 5′ end of the locus. If there is a deletion, its size is <250 bp and does not extend into the neighboring gene(s) (supplemental Fig. S12).

Each mutant was tested relative to the parental wild-type strain CC-4425 for TAG accumulation after transfer to nitrogen-free medium. Both *pdat1-1* and *pdat1-2* mutants show a 25% decrease in TAG content at 48 h. The difference is statistically significant at the 93 and 99% level, respectively (as determined by a two-tailed Student's *t* test), for the 96-h time point (Fig. 8*B*). The impact of the mutation is similar to that noted for the *pdat1* mutant in *Arabidopsis* and the *lro1* mutant in *S. cerevisiae*. For the *nrr1* mutant, we saw a greater impact with a 52% decrease in TAG content at 48 h, which is statistically significant at the 99% confidence level. When we tested the impact of other nutrient deficiencies on TAG accumulation in the

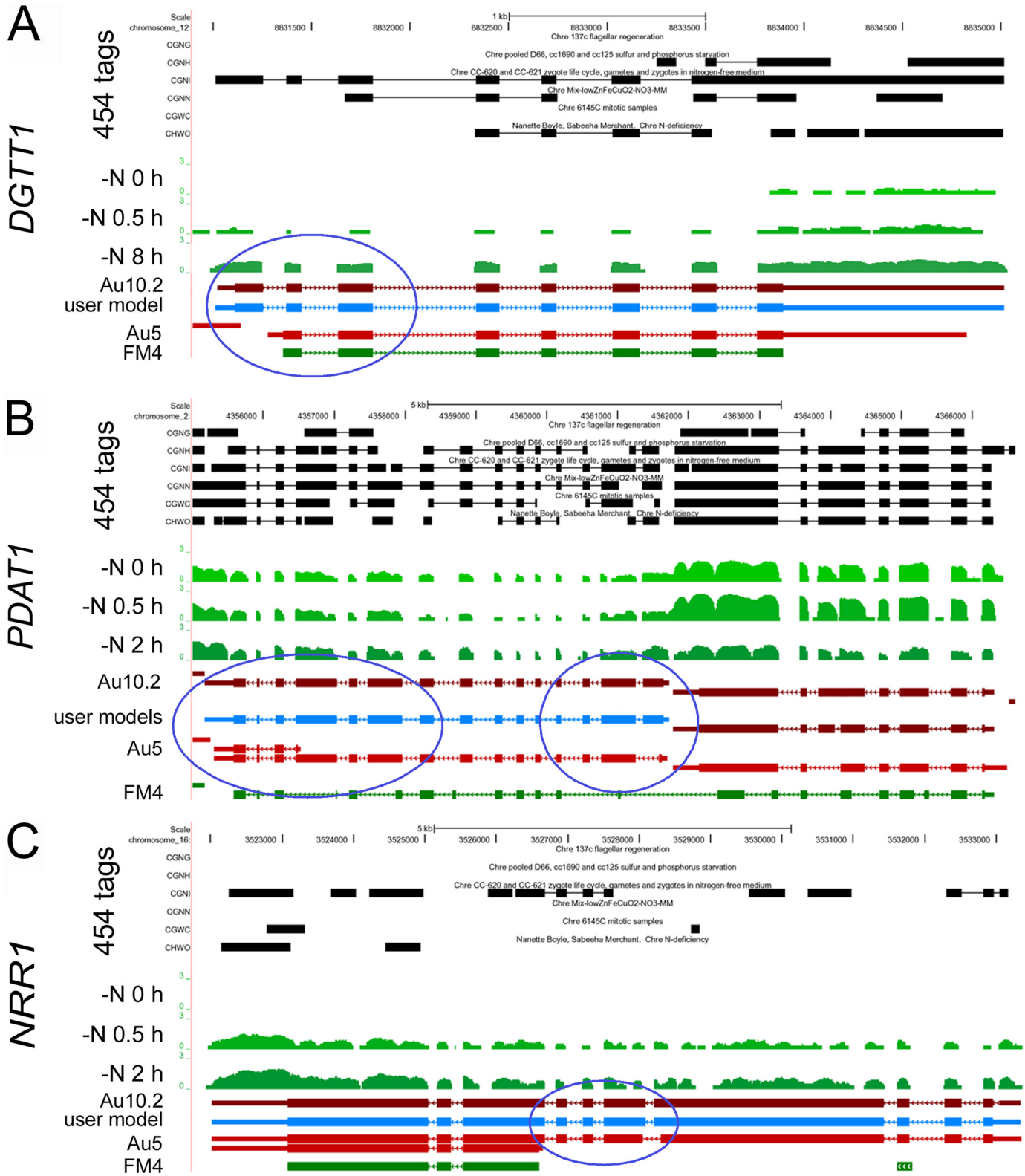

FIGURE 6. **Browser view of *Chlamydomonas DGTT1* (*A*), *PDAT1* (*B*), and *NRR1* (*C*) loci.** The UCSC browser was used to view RNA-Seq coverage. The genome coordinates are shown at the *top*. The next six tracks labeled 454 ESTs represent sequences, collapsed into a single track, from the UCLA/JGI EST project (accession SRX038871). The tracks shown in *green* represent RNA-Seq coverage, on a log scale, for the locus at three time points (0, 0.5, and 2 h) after *Chlamydomonas* cells were transferred to nitrogen-depleted medium. The JGI best gene model for the V4 assembly, FM4, and two different gene models predicted by the Augustus algorithm (Au5 and Au10.2), are shown in *green* and *red,* respectively. *Thick blocks* represent exons, and *thin blocks* represent UTRs, and *arrowed lines* represent introns. RNA-Seq, 454, and EST coverage were used to inform the manual construction of a single gene model at each locus, labeled user model and shown in *blue*. The *PDAT1* gene is on the *left*, and the gene model on the *right* represents an expressed hypothetical protein whose expression is decreased in nitrogen starvation. The *blue circles* highlight new exons suggested by the patterns of RNA-Seq coverage and incorporated by manual curation into revised gene models. The complete data set is available via the UCSC browser on line.

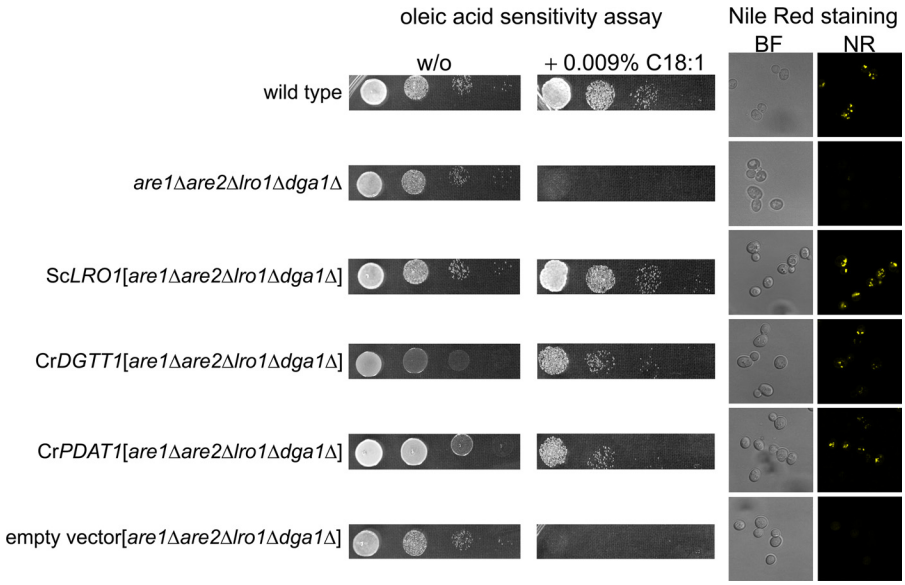

FIGURE 7. **Functional assessment of *DGTT1* and *PDAT1* in yeast.** *Left panel,* oleic acid (C18:1) sensitivity assay of wild type, acyltransferase-deficient yeast, and complemented strains. Yeast strains were grown on agar supplemented with oleic acid (0.009% (w/v)) or not (*w/o*). Wild type, *are1Δare2Δlro1Δdga1Δ* (quadruple mutant lacking all diacylglycerol acyltransferase activity), and mutant strains complemented with *ScLRO1* (encoding PDAT), codon-optimized *CrDGTT1*, codon-optimized *PDAT1*, or an empty vector were grown to an $A_{600} = 1$ diluted 10-fold and plated in serial 10-fold dilutions. *Right,* Nile Red staining of lipid bodies in each yeast strain described above.

mutants, there was no effect (Fig. 8*C*), which confirms that *PDAT1* and *NRR1* are nitrogen starvation-responsive genes with a role in TAG accumulation.

DISCUSSION

Several studies have noted that many algae, when stressed to the point of growth inhibition, accumulate TAGs, a phenomenon of interest to researchers studying biofuels. Work with other organisms, including *S. cerevisiae*, *Arabidopsis*, and mammals, has identified key enzymes, which enable the identification of homologs and orthologs in algae now that genome sequences are available or are in the pipeline (1). Nevertheless, an assessment of the role of these homologs in individual or multiple stress situations requires functional studies. More importantly, if the signaling molecules that initiate the diversion of carbon and lipid metabolism toward TAG accumulation can be identified (referred to as the "lipid trigger"), it would enable the stress-free production of a biofuel precursor without accepting a productivity decline. With these goals, we used a transcriptome-based approach to identify three loci encoding acyltransferases that might be important for TAG accumulation in *Chlamydomonas*, which we are using as a reference organism.

DGAT—There are five genes encoding type-2 DGATs in *Chlamydomonas*; the occurrence of multigene families for these type-2 enzymes is common in the algae (for example, there are three in *Volvox carteri*, two in *Chlorella* sp. NC64A, and seven in *Micromonas pusilla*). Previous work has assigned function to *DGTT2* through *DGTT5* from *Chlamydomonas* via heterologous expression in yeast but not for *DGTT1* (18, 41). Here, we have been able to take advantage of ESTs from nitrogen-deficient cells and RNA-Seq coverage (Fig. 6) to adjust previous gene models. This revealed an extra exon in *DGTT1*, which perhaps facilitated the expression of a functional protein (Fig. 7). *DGTT1* is highly responsive at the level of mRNA abundance to both nitrogen concentration and time after removal of the nitrogen source (Figs. 2 and 6). Orthologs of *Chlamydomonas* DGTT1 in yeast and *Arabidopsis*, Dga1p and DGAT2, respectively, are established as significant contributors to oil accumulation. The yeast *dga1* mutant produces 25% less TAG compared with the wild-type, and *Arabidopsis* DGAT2 is expressed highly in seed where oil accumulates. A phylogenetic tree of DGTT1 and related proteins is presented in supplemental Fig. S13. *DGTT1* has also been reported to be highly induced after 1 day of nitrogen starvation in phototrophically grown *Chlamydomonas* cells (74).

DGAT1 also shows increased expression in nitrogen-deficient cells. The reason that *DGAT1* was not characterized previously is attributed to a gap in the sequence coverage in the version 4 assembly of the genome sequence, which obscures about half the gene model. We reduced this gap substantially but were unable to close it completely even with targeted Sanger sequencing because it is difficult to amplify across the two remaining gaps either using genomic DNA or cDNA as the template. Msanne *et al.* (48) report that *DGAT1* is not responsive to nitrogen starvation when *Chlamydomonas* is grown phototrophically, which may indicate this response is specific to growth on reduced carbon sources, as it is also more highly expressed in seeds of *Arabidopsis* (77). This difference could also be due to strain differences, which have already been noted to impact TAG accumulation (20). These acyltransferases were not identified in a study of the proteome of nitrogen-starved *Thalassiosira pseudonana* (78). In future studies it will be useful to understand the distinction between DGAT1 and DGTT1 with respect to kinetic parameters, substrate specificity, pattern of expression in the life cycle of *Chlamydomonas*, and subcellular location.

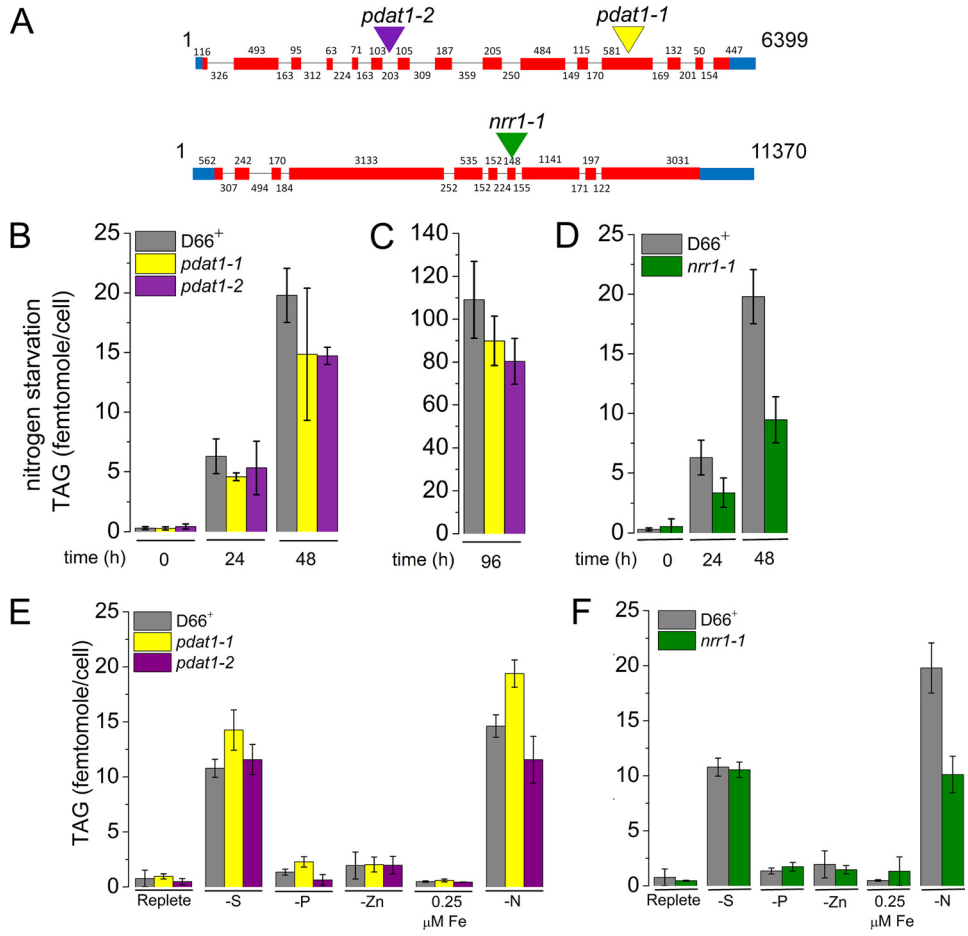

FIGURE 8. **Phenotype of *C. reinhardtii* strains carrying inserts in the *PDAT1* and *NRR1* genes.** *A,* site of insert of *AphVIII* into genomic DNA in the *PDAT1* and *NRR1* mutants is indicated with a *colored triangle* (see supplemental Table 6 for exact position of inset). *B,* TAG content of *pdat1-1* (*yellow*), *pdat1-2* (*purple*), and the parent strain CC-4425 (D66$^+$) (*gray*) measured at 0, 24, and 48 h after nitrogen starvation by quantitative gas chromatography as described under "Experimental Procedures." *C,* TAG content of *pdat1-1* (*yellow*) and *pdat1-2* (*purple*) after 96 h of nitrogen starvation. *D,* TAG content of *nrr1* (*green*) and the parent strain CC-4425 (D66$^+$) (*gray*) measured at 0, 24, and 48 h after nitrogen starvation. *E,* phenotype of *pdat1-1* and *pdat1-2* mutants in other TAG-accumulating conditions ($-PO_4$ and $-SO_4$, 0.25 μM iron, and −zinc). *F,* phenotype of *nrr1-1* mutants in other TAG accumulating conditions ($-PO_4$ and $-SO_4$, 0.25 μM iron, and minus zinc). *Error bars* represent standard deviation from three biological replicates except for *C,* which is from six biological replicates. Two-tailed Student's *t* test on the data indicate that *pdat1-1* and *pdat1-2* are statistically different from the parent strain after 96 h of nitrogen starvation at 93 and 99% confidence levels, respectively; *nrr1-1* is also significantly different at 48 h of nitrogen starvation at 99% confidence.

When we look at the absolute abundance of all DGAT-encoding mRNAs in *Chlamydomonas*, we note that the increase after 48 h of nitrogen starvation is only 62% because two other *DGTT* genes are constitutively expressed at relatively high levels (~20–30 RPKM). This indicates that factors beyond mRNA abundance, such as compartmentalization of enzymes, post-transcriptional regulatory mechanisms that act on the protein(s), and metabolite flux, could contribute to TAG accumulation (1).

What is the source of substrate for the acylation reactions catalyzed by DGATs? Previous studies have provided evidence for fatty acid recycling, and this is consistent with increased expression of lipases in nitrogen-starved cells (18, 42, 73). Some of these are annotated as TAG lipases, which would be counter-intuitive, but they may well be membrane lipid lipases that release fatty acids that are subsequently incorporated into TAGs. Indeed, a recombinant tomato enzyme showed equal activity on TAG as on phosphatidylcholine, and a putative TAG lipase from *Aspergillus oryzae* showed activity on mono- and diacylglycerols as well (79, 80).

PDAT—The acyl-CoA independent pathway, dependent on PDAT1, is less responsive to nitrogen starvation at the level of RNA abundance, which prompted us to use a reverse genetic approach to assess its contribution to TAG accumulation (Fig. 8). The phenotype of *Chlamydomonas pdat1* mutants is very similar to that noted for analogous mutants in yeast, specifically that TAG abundance is decreased but not eliminated. As for DGTT1, PDAT1 is also functional in yeast (Fig. 7); this is relevant because phosphatidylcholine, the preferred substrate of PDAT, is replaced by diacylglycerol trimethylhomoserine in *Chlamydomonas* membranes (26, 81, 82). Interestingly, a recent study showed that *DGAT1*, *DGAT2*, and *PDAT1* genes were induced in nitrogen-deficient *Arabidopsis* seedlings as well, with a pattern (in terms of magnitude) similar to that noted in this study.

Regulators—NRR1, encoding a *SQUAMOSA* promoter-binding protein domain protein (and hence most likely a transcription factor), was identified based on its increased expression within half an hour of nitrogen starvation and its very tight regulation (essentially no RNA in nitrogen-replete cells). The

timing of RNA increase is coincident with the increase in *DGTT1* mRNAs and precedes substantially the appearance of Nile Red staining bodies (Fig. 1). The *nrr1* mutant (likely loss of function because of the presence of a large insert in an exon) loses 50% of its TAG accumulation ability, which speaks to the importance of this regulator in the nitrogen-starvation response. A previous study identified Cre14.g624800 as a candidate regulator, although function was not tested by reverse genetics in that work (83). This gene is up-regulated in our study as well; however, it does not have any conserved domains so the function cannot be predicted. It will be interesting to identify the sought after lipid trigger and test whether its constitutive expression would be sufficient for stimulation of TAG accumulation and lipid body biogenesis.

Acknowledgments—We thank Jane Grimwood (Hudson Alpha) for access to the version 5 assembly prior to release and Sepp Kohlwein (University of Graz) for yeast strains and plasmids. Some sequencing (454 ESTs) was conducted by the United States Department of Energy Joint Genome Institute, which is supported by the Office of Science of the United States Department of Energy under Contract No. DE-AC02-05CH11231.

REFERENCES

1. Merchant, S. S., Kropat, J., Liu, B., Shaw, J., and Warakanont, J. (2012) TAG, You're it! Chlamydomonas as a reference organism for understanding algal triacylglycerol accumulation. *Curr. Opin. Biotechnol.* **23,** 1–12
2. Chisti, Y. (2008) Biodiesel from microalgae beats bioethanol. *Trends Biotechnol.* **26,** 126–131
3. Chisti, Y. (2007) Biodiesel from microalgae. *Biotechnol. Adv.* **25,** 294–306
4. Scott, S. A., Davey, M. P., Dennis, J. S., Horst, I., Howe, C. J., Lea-Smith, D. J., and Smith, A. G. (2010) Biodiesel from algae. Challenges and prospects. *Curr. Opin. Biotechnol.* **21,** 277–286
5. Schenk, P., Thomas-Hall, S., Stephens, E., Marx, U., Mussgnug, J., Posten, C., Kruse, O., and Hankamer, B. (2008) Second generation biofuels. High efficiency microalgae for biodiesel production. *BioEnergy Res.* **1,** 20–43
6. Mata, T. M., Martins, A. A., and Caetano, N. S. (2010) Microalgae for biodiesel production and other applications. A review. *Renewable Sustainable Energy Rev.* **14,** 217–232
7. Griffiths, M., and Harrison, S. (2009) Lipid productivity as a key characteristic for choosing algal species for biodiesel production. *J. Appl. Phycol.* **21,** 493–507
8. Steen, E. J., Kang, Y., Bokinsky, G., Hu, Z., Schirmer, A., McClure, A., Del Cardayre, S. B., and Keasling, J. D. (2010) Microbial production of fatty acid-derived fuels and chemicals from plant biomass. *Nature* **463,** 559–562
9. Waltz, E. (2009) Biotech's green gold? *Nat. Biotechnol.* **27,** 15–18
10. Rosenberg, J. N., Oyler, G. A., Wilkinson, L., and Betenbaugh, M. J. (2008) A green light for engineered algae. Redirecting metabolism to fuel a biotechnology revolution. *Curr. Opin. Biotechnol.* **19,** 430–436
11. Matthew, T., Zhou, W., Rupprecht, J., Lim, L., Thomas-Hall, S. R., Doebbe, A., Kruse, O., Hankamer, B., Marx, U. C., Smith, S. M., and Schenk, P. M. (2009) The metabolome of *Chlamydomonas reinhardtii* following induction of anaerobic H2 production by sulfur depletion. *J. Biol. Chem.* **284,** 23415–23425
12. Wang, Z. T., Ullrich, N., Joo, S., Waffenschmidt, S., and Goodenough, U. (2009) Algal lipid bodies. Stress induction, purification, and biochemical characterization in wild-type and starchless *Chlamydomonas reinhardtii*. *Eukaryot. Cell* **8,** 1856–1868
13. Li, Y., Han, D., Hu, G., Dauvillee, D., Sommerfeld, M., Ball, S., and Hu, Q. (2010) *Chlamydomonas* starchless mutant defective in ADP-glucose pyrophosphorylase hyper-accumulates triacylglycerol. *Metab. Eng.* **12,** 387–391
14. Li, Y., Han, D., Hu, G., Sommerfeld, M., and Hu, Q. (2010) Inhibition of starch synthesis results in overproduction of lipids in *Chlamydomonas reinhardtii*. *Biotechnol. Bioeng.* **107,** 258–268
15. Weers, P. M., and Gulati, R. D. (1997) Growth and reproduction of *Daphnia galeata* in response to changes in fatty acids, phosphorus, and nitrogen in *Chlamydomonas reinhardtii*. *Limnol. Oceanogr.* **42,** 1584–1589
16. Hu, Q., Sommerfeld, M., Jarvis, E., Ghirardi, M., Posewitz, M., Seibert, M., and Darzins, A. (2008) Microalgal triacylglycerols as feedstocks for biofuel production: perspectives and advances. *Plant J.* **54,** 621–639
17. Work, V. H., Radakovits, R., Jinkerson, R. E., Meuser, J. E., Elliott, L. G., Vinyard, D. J., Laurens, L. M., Dismukes, G. C., and Posewitz, M. C. (2010) Increased lipid accumulation in the *Chlamydomonas reinhardtii* sta7-10 starchless isoamylase mutant and increased carbohydrate synthesis in complemented strains. *Eukaryot. Cell* **9,** 1251–1261
18. Miller, R., Wu, G., Deshpande, R. R., Vieler, A., Gaertner, K., Li, X., Moellering, E. R., Zauner, S., Cornish, A., Liu, B., Bullard, B., Sears, B. B., Kuo, M. H., Hegg, E. L., Shachar-Hill, Y., Shiu, S. H., and Benning, C. (2010) Changes in transcript abundance in *Chlamydomonas reinhardtii* following nitrogen deprivation predict diversion of metabolism. *Plant Physiol.* 110.165159
19. Moellering, E. R., and Benning, C. (2010) RNA interference silencing of a major lipid droplet protein affects lipid droplet size in *Chlamydomonas reinhardtii*. *Eukaryot. Cell* **9,** 97–106
20. Goodson, C., Roth, R., Wang, Z. T., and Goodenough, U. (2011) Structural correlates of cytoplasmic and chloroplast lipid body synthesis in *Chlamydomonas reinhardtii* and stimulation of lipid body production with acetate boost. (2011) *Eukaryot. Cell* **10,** 1592–1606
21. Kropat, J., Hong-Hermesdorf, A., Casero, D., Ent, P., Castruita, M., Pellegrini, M., Merchant, S. S., and Malasarn, D. (2011) A revised mineral supplement increase biomass and growth rate in *Chlamydomonas reinhardtii*. *Plant J.* **66,** 770–780
22. Siaut, M., Cuiné, S., Cagnon, C., Fessler, B., Nguyen, M., Carrier, P., Beyly, A., Beisson, F., Triantaphylidès, C., Li-Beisson, Y., and Peltier, G. (2011) Oil accumulation in the model green alga *Chlamydomonas reinhardtii*. Characterization, variability between common laboratory strains, and relationship with starch reserves. *BMC Biotechnol.* **11,** 7
23. Zhekisheva, M., Boussiba, S., Khozin-Goldberg, I., Zarka, A., and Cohen, Z. (2002) Accumulation of oleic acid in *Haematococcus pluvialis* (*Chlorophyceae*) under nitrogen starvation or high light is correlated with that of astaxanthin esters. *J. Phycol.* **38,** 325–331
24. Merchant, S. S., Prochnik, S. E., Vallon, O., Harris, E. H., Karpowicz, S. J., Witman, G. B., Terry, A., Salamov, A., Fritz-Laylin, L. K., Maréchal-Drouard, L., Marshall, W. F., Qu, L. H., Nelson, D. R., Sanderfoot, A. A., Spalding, M. H., Kapitonov, V. V., Ren, Q., Ferris, P., Lindquist, E., Shapiro, H., Lucas, S. M., Grimwood, J., Schmutz, J., Cardol, P., Cerutti, H., Chanfreau, G., Chen, C. L., Cognat, V., Croft, M. T., Dent, R., Dutcher, S., Fernández, E., Fukuzawa, H., González-Ballester, D., González-Halphen, D., Hallmann, A., Hanikenne, M., Hippler, M., Inwood, W., Jabbari, K., Kalanon, M., Kuras, R., Lefebvre, P. A., Lemaire, S. D., Lobanov, A. V., Lohr, M., Manuell, A., Meier, I., Mets, L., Mittag, M., Mittelmeier, T., Moroney, J. V., Moseley, J., Napoli, C., Nedelcu, A. M., Niyogi, K., Novoselov, S. V., Paulsen, I. T., Pazour, G., Purton, S., Ral, J. P., Riaño-Pachon, D. M., Riekhof, W., Rymarquis, L., Schroda, M., Stern, D., Umen, J., Willows, R., Wilson, N., Zimmer, S. L., Allmer, J., Balk, J., Bisova, K., Chen, C. J., Elias, M., Gendler, K., Hauser, C., Lamb, M. R., Ledford, H., Long, J. C., Minagawa, J., Page, M. D., Pan, J., Pootakham, W., Roje, S., Rose, A., Stahlberg, E., Terauchi, A. M., Yang, P., Ball, S., Bowler, C., Dieckmann, C. L., Gladyshev, V. N., Green, P., Jorgensen, R., Mayfield, S., Mueller-Roeber, B., Rajamani, S., Sayre, R. T., Brokstein, P., Dubchak, I., Goodstein, D., Hornick, L., Huang, Y. W., Jhaveri, J., Luo, Y., Martinez, D., Ngau, W. C., Otillar, B., Poliakov, A., Porter, A., Szajkowski, L., Werner, G., Zhou, K., Grigoriev, I. V., Rokhsar, D. S., and Grossman, A. R. (2007) The *Chlamydomonas genome* reveals the evolution of key animal and plant functions. *Science* **318,** 245–250
25. Wijffels, R. H., and Barbosa, M. J. (2010) An outlook on microalgal biofuels. *Science* **329,** 796–799
26. Giroud, C., Gerber, A., and Eichenberger, W. (1988) Lipids of *Chlamydomonas reinhardtii*. Analysis of molecular species and intracellular

sites(s) of biosynthesis. *Plant Cell Physiol.* **29,** 587–595
27. Riekhof, W. R., Sears, B. B., and Benning, C. (2005) Annotation of genes involved in glycerolipid biosynthesis in *Chlamydomonas reinhardtii*. Discovery of the betaine lipid synthase BTA1Cr. *Eukaryot. Cell* **4,** 242–252
28. Cases, S., Smith, S. J., Zheng, Y. W., Myers, H. M., Lear, S. R., Sande, E., Novak, S., Collins, C., Welch, C. B., Lusis, A. J., Erickson, S. K., and Farese, R. V. (1998) Identification of a gene encoding an acyl CoA:diacylglycerol acyltransferase, a key enzyme in triacylglycerol synthesis. *Proc. Natl. Acad. Sci. U.S.A.* **95,** 13018–13023
29. Lardizabal, K. D., Mai, J. T., Wagner, N. W., Wyrick, A., Voelker, T., and Hawkins, D. J. (2001) DGAT2 is a new diacylglycerol acyltransferase gene family. Purification, cloning, and expression in insect cells of two polypeptides from *Mortierella ramanniana* with diacylglycerol acyltransferase activity. *J. Biol. Chem.* **276,** 38862–38869
30. Stymne, S., and Stobart, A. K. (1987) in *The Biochemistry of Plants* (Stumpf, P. K., ed) pp. 175–214, Academic Press, New York
31. Lacey, D. J., and Hills, M. J. (1996) Heterogeneity of the endoplasmic reticulum with respect to lipid synthesis in developing seeds of the *Brassica napus* L. *Planta* **199,** 545–551
32. Stobart, A. K., Stymne, S., and Höglund, S. (1986) Safflower microsomes catalyze oil accumulation *in vitro*. A model system. *Planta* **169,** 33–37
33. Shockey, J. M., Gidda, S. K., Chapital, D. C., Kuan, J. C., Dhanoa, P. K., Bland, J. M., Rothstein, S. J., Mullen, R. T., and Dyer, J. M. (2006) Tung tree DGAT1 and DGAT2 have nonredundant functions in triacylglycerol biosynthesis and are localized to different subdomains of the endoplasmic reticulum. *Plant Cell* **18,** 2294–2313
34. Li, R., Yu, K., and Hildebrand, D. (2010) DGAT1, DGAT2, and PDAT expression in seeds and other tissues of epoxy and hydroxy fatty acid accumulating plants. *Lipids* **45,** 145–157
35. Banilas, G., Karampelias, M., Makariti, I., Kourti, A., and Hatzopoulos, P. (2011) The olive *DGAT2* gene is developmentally regulated and shares overlapping but distinct expression patterns with DGAT1. *J. Exp. Bot.* **62,** 521–532
36. Stone, S. J., Myers, H. M., Watkins, S. M., Brown, B. E., Feingold, K. R., Elias, P. M., and Farese, R. V. (2004) Lipopenia and skin barrier abnormalities in DGAT2-deficient mice. *J. Biol. Chem.* **279,** 11767–11776
37. Saha, S., Enugutti, B., Rajakumari, S., and Rajasekharan, R. (2006) Cytosolic triacylglycerol biosynthetic pathway in oilseeds. Molecular cloning and expression of peanut cytosolic diacylglycerol acyltransferase. *Plant Physiol.* **141,** 1533–1543
38. Peng, F. Y., and Weselake, R. J. (2011) Gene coexpression clusters and putative regulatory elements underlying seed storage reserve accumulation in *Arabidopsis*. *BMC Genomics* **12,** 286
39. Sandager, L., Gustavsson, M. H., Ståhl, U., Dahlqvist, A., Wiberg, E., Banas, A., Lenman, M., Ronne, H., and Stymne, S. (2002) Storage lipid synthesis is nonessential in yeast. *J. Biol. Chem.* **277,** 6478–6482
40. Oelkers, P., Cromley, D., Padamsee, M., Billheimer, J. T., and Sturley, S. L. (2002) The *DGA1* gene determines a second triglyceride synthetic pathway in yeast. *J. Biol. Chem.* **277,** 8877–8881
41. Benning, C., Miller, R., and Moellering, E. R. (2010) Enzyme-directed oil biosynthesis in microalgae, Michigan State University Board of Trustees
42. Nguyen, H. M., Baudet, M., Cuiné, S., Adriano, J. M., Barthe, D., Billon, E., Bruley, C., Beisson, F., Peltier, G., Ferro, M., and Li-Beisson, Y. (2011) Proteomic profiling of oil bodies isolated from the unicellular green microalga *Chlamydomonas reinhardtii*, with focus on proteins involved in lipid metabolism. *Proteomics* **11,** 4266–4273
43. Pollock, S. V., Colombo, S. L., Prout, D. L., Jr., Godfrey, A. C., and Moroney, J. V. (2003) Rubisco activase is required for optimal photosynthesis in the green alga *Chlamydomonas reinhardtii* in a low CO_2 atmosphere. *Plant Physiol.* **133,** 1854–1861
44. Schnell, R. A., and Lefebvre, P. A. (1993) Isolation of the *Chlamydomonas* regulatory gene NIT2 by transposon tagging. *Genetics* **134,** 737–747
45. Harris, E. H. (1989) *The Chlamydomonas Sourcebook: A Comprehensive Guide to Biology and Laboratory Use*, Academic Press, Inc., San Diego
46. Quisel, J. D., Wykoff, D. D., and Grossman, A. R. (1996) Biochemical characterization of the extracellular phosphatases produced by phosphorus-deprived *Chlamydomonas reinhardtii*. *Plant Physiol.* **111,** 839–848
47. Moseley, J., Quinn, J., Eriksson, M., and Merchant, S. (2000) The *Crd1* gene encodes a putative di-iron enzyme required for photosystem I accumulation in copper deficiency and hypoxia in *Chlamydomonas reinhardtii*. *EMBO J.* **19,** 2139–2151
48. González-Ballester, D., Casero, D., Cokus, S., Pellegrini, M., Merchant, S. S., and Grossman, A. R. (2010) RNA-seq analysis of sulfur-deprived *Chlamydomonas* cells reveals aspects of acclimation critical for cell survival. *Plant Cell* **22,** 2058–2084
49. Moseley, J. L., Allinger, T., Herzog, S., Hoerth, P., Wehinger, E., Merchant, S., and Hippler, M. (2002) Adaptation to Fe deficiency requires remodeling of the photosynthetic apparatus. *EMBO J.* **21,** 6709–6720
50. Allen, M. D., del Campo, J. A., Kropat, J., and Merchant, S. S. (2007) FEA1, FEA2, and FRE1, encoding two homologous secreted proteins and a candidate ferrireductase, are expressed coordinately with FOX1 and FTR1 in iron-deficient *Chlamydomonas reinhardtii*. *Eukaryot. Cell* **6,** 1841–1852
51. Hill, K. L., Li, H. H., Singer, J., and Merchant, S. (1991) Isolation and structural characterization of the *Chlamydomonas reinhardtii* gene for cytochrome c_6. Analysis of the kinetics and metal specificity of its copper-responsive expression. *J. Biol. Chem.* **266,** 15060–15067
52. Quinn, J. M., and Merchant, S. (1998) in *Methods in Enzymology* (Lee, M., ed) pp. 263–279, Academic Press, New York
53. Langmead, B., Trapnell, C., Pop, M., and Salzberg, S. (2009) Ultrafast and memory-efficient alignment of short DNA sequences to the human genome. *Genome Biol.* **10,** R25
54. Mortazavi, A., Williams, B. A., McCue, K., Schaeffer, L., and Wold, B. (2008) Mapping and quantifying mammalian transcriptomes by RNA-Seq. *Nat. Meth.* **5,** 621–628
55. Xie, Z., and Merchant, S. (1996) The plastid-encoded *ccsA* gene is required for heme attachment to chloroplast *c*-type cytochromes. *J. Biol. Chem.* **271,** 4632–4639
56. Depège, N., Bellafiore, S., and Rochaix, J. D. (2003) Role of chloroplast protein kinase Stt7 in LHCII phosphorylation and state transition in *Chlamydomonas*. *Science* **299,** 1572–1575
57. Feinberg, A. P., and Vogelstein, B. (1983) A technique for radiolabeling DNA restriction endonuclease fragments to high specific activity. *Anal. Biochem.* **132,** 6–13
58. Ramakers, C., Ruijter, J. M., Deprez, R. H., and Moorman, A. F. (2003) Assumption-free analysis of quantitative real time polymerase chain reaction (PCR) data. *Neurosci. Lett.* **339,** 62–66
59. Ruijter, J. M., Ramakers, C., Hoogaars, W. M., Karlen, Y., Bakker, O., van den Hoff, M. J., and Moorman, A. F. (2009) Amplification efficiency. Linking base line and bias in the analysis of quantitative PCR data. *Nucleic Acids Res.* **37,** e45
60. Bustin, S. A., Benes, V., Garson, J. A., Hellemans, J., Huggett, J., Kubista, M., Mueller, R., Nolan, T., Pfaffl, M. W., Shipley, G. L., Vandesompele, J., and Wittwer, C. T. (2009) The MIQE guidelines: minimum information for publication of quantitative real time PCR experiments. *Clin. Chem.* **55,** 611–622
61. Simpson, J. T., Wong, K., Jackman, S. D., Schein, J. E., Jones, S. J., and Birol, I. (2009) ABySS. A parallel assembler for short read sequence data. *Genome Res.* **19,** 1117–1123
62. Wu, T. D., and Watanabe, C. K. (2005) GMAP. A genomic mapping and alignment program for mRNA and EST sequences. *Bioinformatics* **21,** 1859–1875
63. Kent, W. J., Sugnet, C. W., Furey, T. S., Roskin, K. M., Pringle, T. H., Zahler, A. M., and Haussler, D. (2002) The human genome browser at UCSC. *Genome Res.* **12,** 996–1006
64. Robinson, J. T., Thorvaldsdóttir, H., Winckler, W., Guttman, M., Lander, E. S., Getz, G., and Mesirov, J. P. (2011) Integrative genomics viewer. *Nat. Biotechnol.* **29,** 24–26
65. Rossak, M., Schäfer, A., Xu, N., Gage, D. A., and Benning, C. (1997) Accumulation of sulfoquinovosyl-1-*O*-dihydroxyacetone in a sulfolipid-deficient mutant of *Rhodobacter sphaeroides* inactivated in sqdC. *Arch. Biochem. Biophys.* **340,** 219–230
66. Sizova, I., Fuhrmann, M., and Hegemann, P. (2001) A *Streptomyces rimosus* aphVIII gene coding for a new type phosphotransferase provides stable antibiotic resistance to *Chlamydomonas reinhardtii*. *Gene* **277,** 221–229
67. Pootakham, W., Gonzalez-Ballester, D., and Grossman, A. R. (2010) Identification and regulation of plasma membrane sulfate transporters in

Chlamydomonas. *Plant Physiol.* **153,** 1653–1668
68. Gonzalez-Ballester, D., Pootakham, W., Mus, F., Yang, W., Catalanotti, C., Magneschi, L., de Montaigu, A., Higuera, J. J., Prior, M., Galván, A., Fernandez, E., and Grossman, A. R. (2011) Reverse genetics in *Chlamydomonas*. A platform for isolating insertional mutants. *Plant Methods* **7,** 24
69. Sambrook, J., Fritsch, E., and Maniatis, T. (1989) *Molecular Cloning: A Laboratory Manual*, Cold Spring Harbor Laboratory Press, Cold Spring Harbor, NY
70. James, G. O., Hocart, C. H., Hillier, W., Chen, H., Kordbacheh, F., Price, G. D., and Djordjevic, M. A. (2011) Fatty acid profiling of *Chlamydomonas reinhardtii* under nitrogen deprivation. *Bioresour. Technol.* **102,** 3343–3351
71. Moellering, E. R., Miller, R., and Benning, C. (2009) in *Lipids in Photosynthesis: Essential and Regulatory Functions* (Wada, H., and Murata, N., eds) pp. 139–155, Spring Science + Business, Berlin
72. Riekhof, W. R., and Benning, C. (2009) in *The Chlamydomonas Sourcebook* (Harris, E. H., ed) pp. 41–68, Elsevier Science Publishers B.V., Amsterdam
73. Fan, J., Andre, C., and Xu, C. (2011) A chloroplast pathway for the de novo biosynthesis of triacylglycerol in *Chlamydomonas reinhardtii*. *FEBS Lett.* **585,** 1985–1991
74. Msanne, J., Xu, D., Konda, A. R., Casas-Mollano, J. A., Awada, T., Cahoon, E. B., and Cerutti, H. (2012) Metabolic and gene expression changes triggered by nitrogen deprivation in the photoautotrophically grown microalgae *Chlamydomonas reinhardtii* and *Coccomyxa* sp. C-169. **75,** 50–59
75. Petschnigg, J., Wolinski, H., Kolb, D., Zellnig, G., Kurat, C. F., Natter, K., and Kohlwein, S. D. (2009) Good fat, essential cellular requirements for triacylglycerol synthesis to maintain membrane homeostasis in yeast. *J. Biol. Chem.* **284,** 30981–30993
76. Lockshon, D., Surface, L. E., Kerr, E. O., Kaeberlein, M., and Kennedy, B. K. (2007) The sensitivity of yeast mutants to oleic acid implicates the peroxisome and other processes in membrane function. *Genetics* **175,** 77–91
77. Zhang, M., Fan, J., Taylor, D. C., and Ohlrogge, J. B. (2009) DGAT1 and PDAT1 acyltransferases have overlapping functions in *Arabidopsis triacylglycerol* biosynthesis and are essential for normal pollen and seed development. *Plant Cell* **21,** 3885–3901
78. Hockin, N. L., Mock, T., Mulholland, F., Kopriva, S., and Malin, G. (2012) The response of diatom central carbon metabolism to nitrogen starvation is different from that of green algae and higher plants. *Plant Physiol.* **158,** 299–312
79. Matsui, K., Fukutomi, S., Ishii, M., and Kajiwara, T. (2004) A tomato lipase homologous to DAD1 (LeLID1) is induced in post-germinative growing stage and encodes a triacylglycerol lipase. *FEBS Lett.* **569,** 195–200
80. Toida, J., Arikawa, Y., Kondou, K., Fukuzawa, M., and Sekiguchi, J. (1998) Purification and characterization of triacylglycerol lipase from *Aspergillus oryzae*. *Biosci. Biotechnol. Biochem.* **62,** 759–763
81. Vieler, A., Wilhelm, C., Goss, R., Süss, R., and Schiller, J. (2007) The lipid composition of the unicellular green alga *Chlamydomonas reinhardtii* and the diatom *Cyclotella meneghiniana* investigated by MALDI-TOF MS and TLC. *Chem. Phys. Lipids* **150,** 143–155
82. Harris, E. H. (2009) *The Chlamydomonas Sourcebook,* 2 Ed., Elsevier, Amsterdam
83. Yohn, C., Mendez, M., Behnke, C., and Brand, A. (November 8, 2011) Stress-induced Lipid Trigger Organization, Sapphire Energy, U.S. Patent no. US 2011 023406